



# Population genetic structure of the deep-sea precious red coral *Hemicorallium laauense* along the Hawaiian Ridge

Nicole B. Morgan<sup>1</sup> · Julia Andrews<sup>1</sup> · Amy R. Baco<sup>1</sup>

Received: 23 April 2023 / Accepted: 17 August 2023

© The Author(s), under exclusive licence to Springer-Verlag GmbH Germany, part of Springer Nature 2023

## Abstract

The deep-sea precious red coral *Hemicorallium laauense* has long been overharvested in the North Pacific for the jewelry and curio trades. An understanding of the population structure and connectivity of these octocorals has been limited due to the difficulty of sampling and taxonomic challenges within the Family Corallidae. We report on population genetics of 270 *H. laauense* individuals from 16 populations throughout the Main Hawaiian Islands (MHI) and the Northwestern Hawaiian Islands (NWHI) using nine microsatellite loci. Observed heterozygosity (0.69–0.85) was generally lower than expected heterozygosity (0.71–0.85) except for the population at Twin Banks. Moderate  $F_{IS}$  values (0.01–0.20) were present in nearly half of the populations. Global  $G'_{ST}$  (0.166) and pairwise values were moderate to high (−0.003 to 0.489).  $G'_{ST}$  values also show moderate genetic structuring among populations within seamounts (0.12–0.22) for populations separated by as little as 3 km. DAPC indicated separation of the MHI from the NWHI, but two NWHI sites fall into the MHI clusters and samples from Ka'ena Point (an MHI site) appear to form their own cluster. Membership assignments showed moderate admixture between some locations, while three locations showed almost no admixture. Within-seamount admixture was surprisingly limited for populations on the same seamount. A pattern of isolation by distance, with exchange primarily among adjacent seamounts, was supported by MIGRATE results but not by Mantel tests. These results suggest a mixed pattern of connectivity, with some distant locations well connected and others more isolated. The inconsistent connectivity of these corals is likely amplified by their patchy distributions.

**Keywords** Population structure · Deep-sea corals · Seamount · Connectivity · Octocorals

## Introduction

In many deep-sea hard substrate habitats, octocorals are important ecosystem engineers (Genin et al. 1986; Mortensen and Buhl-Mortensen 2004; Stocks 2004; Baco 2007; Rogers et al. 2007; Buhl-Mortensen et al. 2009; Baker et al. 2012) that can form dense gardens and provide shelter and food for numerous other species (Stocks 2004; Buhl-Mortensen et al. 2009; Baillon et al. 2012; Pham et al. 2015). This is especially true on seamounts in the North Pacific, where octocorals were expected to be

the only structure-forming corals (Guinotte et al. 2006; Baco 2007; Baco et al. 2017; Kennedy et al. 2019), until the recent discovery of scleractinian reefs in the Northwest Hawaiian Islands (Baco et al. 2017). Seamounts can be isolated habitats, separated from other hard substrate features by distance, soft substrate habitats, currents, and/or water mass changes that prevent larvae from dispersing between features (Genin et al. 1989; Stocks and Hart 2007; Sautya et al. 2011). Seamounts are also known to have very patchy community structure with fragmented species distributions (Lundsten et al. 2009; McClain et al. 2010; Williams et al. 2010; Bo et al. 2011; Sautya et al. 2011; Long and Baco 2014; Schlacher et al. 2014; Thresher et al. 2014; McClain and Lundsten 2015; Morgan et al. 2015, 2019; Bell et al. 2016; Mejía-Mercado et al. 2019) which enhances the likelihood of isolation of populations.

Deep-water octocorals often have life histories that include slow growth and long lifespans (Andrews et al. 2002, 2009; Roark et al. 2005, 2009). These life history traits as

---

Responsible Editor: S. Harii.

---

✉ Amy R. Baco  
abacotaylor@fsu.edu

<sup>1</sup> Department of Earth, Ocean, and Atmospheric Science, Florida State University, 1011 Academic Way, Tallahassee, FL 32304, USA

well as their roles as critical habitat for other deep-sea species (Stocks 2004; Buhl-Mortensen et al. 2009; Henderson et al. 2020) have resulted in deep-sea octocoral communities being designated as Vulnerable Marine Ecosystems (VMEs) (Thompson et al. 2016) and as Ecologically or Biologically Significant Areas (EBSAs) (CBD 2011). Seamounts as a whole are also categorized as VMEs according to the UNGA resolution 61/105 (UN General Assembly 2007) due to the numerous species that are found on seamounts with similarly vulnerable life history traits. Regulatory bodies have a requirement to enact protection of VMEs and EBSAs within their purview but having better knowledge of the connectivity of these populations would greatly improve management efforts.

Connectivity for deep-sea octocorals is still not well known, as only a handful of studies, discussed below, have been published. Deep and mesophotic species have shown significant genetic differentiation over small geographic scales (5–20 km) and small depth changes (20–100 m) (Quattrini et al. 2015; Pérez-Portela et al. 2016). In contrast to these studies showing high differentiation, other studies show higher connectivity between distant populations of octocorals over scales of 50–300 km and depth gradients of 600 m (Wright et al. 2015; Holland et al. 2017; Yesson et al. 2018). With so few connectivity studies done for deep-water and mesophotic octocorals, and with such disparate results, it is difficult to derive a general pattern of genetic connectivity by distance and/or depth gradients.

A common and important structure-forming octocoral in the North Pacific is *Hemicorallium laauense* Bayer 1956, in the family Coralliidae (Parrish and Baco 2007; Parrish et al. 2015). It can be found throughout the Pacific Ocean at depths of 300–2000 m, (though most records are between 300 and 900 m) (OBIS 2021). The genera of the family Coralliidae were recently revised and the genus *Hemicorallium* was resurrected and reorganized, with several species that were once in the genus *Corallium* moved into *Hemicorallium* (Ardila et al. 2012; Figueira and Baco 2014; Tu et al. 2016). These revisions also showed that the species *Hemicorallium laauense* is likely a complex of at least two species (Tu et al. 2016). *H. laauense* is known to be slow growing, long lived, slow maturing, and to have size-dependent fecundity (Grigg 2002; Torrents et al. 2005; Roark et al. 2006). Little data exist on the reproductive strategy for *Hemicorallium* (Waller and Baco 2007). *Corallium rubrum* from the Mediterranean, in the same family, are known to brood their larvae and release developed planulae which are negatively gravitactic (Santangelo et al. 2003; Tsounis et al. 2006). In contrast, confamilial *Pleurocorallium secundum* are periodic spawners that are thought to release planktotrophic larvae (Waller and Baco 2007).

*Hemicorallium laauense*, along with numerous other species of Coralliidae, has been heavily harvested throughout

the Hawaiian Archipelago and into the Emperor Seamount Chain, for the jewelry and curio trades (Grigg 1976, 1993, 2002; Parrish and Baco 2007; Parrish et al. 2009; Bruckner 2016), which has likely had a significant toll on the genetic diversity of these populations. The ability of the harvested populations to recover is not well known, as the connectivity between coral gardens within the Hawaiian Archipelago is not well defined. An earlier study found high levels of genetic diversity for *H. laauense* across 12 sites in the Hawaiian Archipelago, yet significant heterozygosity deficiencies, suggesting inbreeding depression for many populations (Baco and Shank 2005). The study also found varying levels of genetic differentiation, with most differences occurring between islands separated by 300–1000 km, but differences were also found within the Makapu'u coral bed less than 2 km apart (Baco and Shank 2005). Surprisingly, some populations separated by nearly 1000 km did not show differentiation, which may suggest episodic long-distance migration between features.

*Corallium rubrum*, in the same family, is also known to have population genetic structuring throughout the Mediterranean, at scales as small as tens of meters within two populations off the Italian coast (Costantini et al. 2007; Ledoux et al. 2010), and at larger scales between populations separated by hundreds of kilometers (Ledoux et al. 2010; Costantini et al. 2011) and between basins of the Mediterranean Sea (Costantini and Abbiati 2016). *Corallium rubrum* also shows significant heterozygote deficiencies and a decrease in genetic diversity with depth, which are likely due to their brooding reproductive strategy (Costantini et al. 2007, 2011). Off the coast of Kochi, Japan *Corallium japonicum* populations assessed by genome-wide single-nucleotide polymorphisms showed local population structure and a population break at 11 km of distance (Takata et al. 2021).

Studies of population genetic structure for shallow-water marine species in the Hawaiian Archipelago may provide additional insights into connectivity patterns of deeper species on the same seamounts. Toonen et al. (2011) found four barriers to dispersal that broke the Main Hawaiian Islands (MHI) into three regions and the Northwestern Hawaiian Islands (NWHI) into two regions of dispersal. Their study also showed very few species showed a pattern of isolation by distance (IBD), even though the stepping-stone geographic layout of the Archipelago was expected to enhance IBD, and in fact distance was a poor predictor of connectivity (Toonen et al. 2011). There is also evidence that multiple models of genetic structuring can be found within the Archipelago, and that the type of structuring may not easily be predicted by life histories (Selkoe et al. 2014). In general, Selkoe et al. (2014) found regional structuring was the most common pattern for the species examined, and IBD the least common, which further supported the genetic breaks found in Toonen et al. (2011). Most recently, biophysical

modeling for dispersal across the Archipelago found most features were likely to be dominated by self-recruitment, and that most external recruitment would move propagules from the MHI to the NWHI rather than in the reverse direction as had been hoped (Wren et al. 2016). These models contrast with the genetic data in that they support IBD patterns. However, the expected breaks in dispersal match well with previous studies that separate the MHI from the NWHI and separate the westernmost atolls in the NWHI from more central features (Wren et al. 2016).

The challenges of delimiting the species within *Hemicorallium* as well as the lack of background population structure data for *H. laauense* make predicting connectivity patterns difficult, due to difficulty in defining any species boundaries, which in turn can hamper effective management when considering anthropogenic stressors. The previous studies on connectivity on shallow reef-associated species in the Hawaiian Archipelago and on species and population delimitation in members of the family Corallidae highlight the complex factors that may influence this species populations genetics. To gain clearer insights into the population

connectivity of this deep-sea coral, we use microsatellites from 16 populations of *Hemicorallium laauense* throughout the Hawaiian Archipelago to test the hypothesis of limited connectivity between seamounts. We test for (1) a pattern of IBD with increasing distance between seamounts over large spatial scales, (2) to see if instead there is a more regional structuring between the MHI and the NWHI; and finally, (3) we test for finer-scale genetic structuring within three seamounts with multiple populations.

## Methods

### Sampling locations

*H. laauense* samples were collected by the submersibles *Pisces IV* and *Pisces V* during cruises onboard the *RV Ka'imikai-O-Kanaloa* in 1998, 2000, 2002, 2003, 2004, 2016, and 2017 at a total of 16 locations ranging in depth from 300 to 650 m (Fig. 1; Table 1). In general, target locations for this study have no history of coral harvesting with

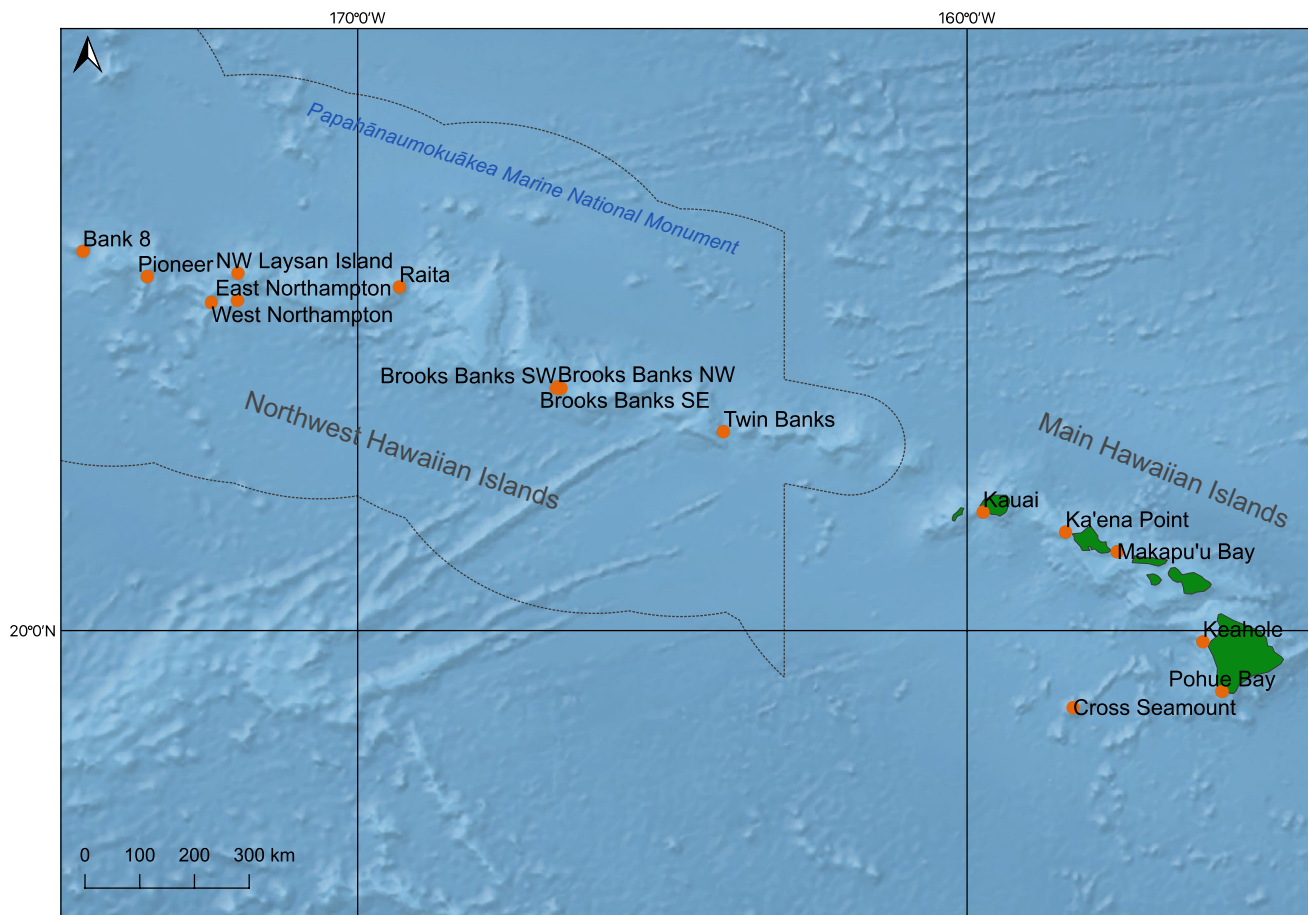


**Fig. 1** Map of sites within the Hawaiian Archipelago. Land forms are shown in green, and the boundary of the Papahānaumokuākea Marine National Monument is shown as a thin black line

**Table 1** By-site metrics

| Site             | Latitude N | Longitude E | Depth range (m) | N  | NA  | NPA | Multilocus genotype | Allelic richness | Zahl's | $N_e^*$  | $N_e$ 95% CI*       | $F_{IS}^*$ | $H_e^*$ | $H_o^*$ |
|------------------|------------|-------------|-----------------|----|-----|-----|---------------------|------------------|--------|----------|---------------------|------------|---------|---------|
| Bank 8           | 26.226     | 174.509     | 512–547         | 14 | 114 | 3   | 14                  | 4.48             | 2.63   | 18.7     | 9.2–31.6            | 0.06       | 0.85    | 0.84    |
| Brooks Banks NW  | 23.997     | 166.716     | 417–442         | 17 | 102 | 0   | 17                  | 4.23             | 2.40   | 13       | 4.2–26.6            | 0.20       | 0.83    | 0.69    |
| Brooks Banks SE  | 23.976     | 166.663     | 454–462         | 15 | 103 | 1   | 15                  | 4.19             | 2.26   | 26.6     | 6.4–60.9            | 0.13       | 0.79    | 0.70    |
| Brooks Banks SW  | 23.977     | 166.739     | 448–590         | 16 | 116 | 2   | 16                  | 4.41             | 2.52   | 26.8     | 8.7–54.9            | 0.13       | 0.84    | 0.75    |
| Cross seamount   | 18.733     | 158.259     | 404–427         | 20 | 130 | 4   | 20                  | 4.47             | 2.47   | $\infty$ | $\infty$ – $\infty$ | 0.10       | 0.84    | 0.77    |
| East Northampton | 25.419     | 171.976     | 501–669         | 25 | 137 | 6   | 25                  | 4.39             | 2.49   | 62.5     | 0.1–313.7           | 0.01       | 0.84    | 0.85    |
| Ka'ena Point     | 21.617     | 158.383     | 417–550         | 7  | 60  | 0   | 7                   | 3.83             | 1.97   | 6.9      | 4.3–10.1            | 0.09       | 0.74    | 0.73    |
| Kaua'i           | 21.944     | 159.736     | 481–533         | 20 | 119 | 2   | 20                  | 4.33             | 2.34   | 22       | 8.5–41.8            | 0.09       | 0.82    | 0.76    |
| Keahole Point    | 19.815     | 156.129     | 385–410         | 26 | 143 | 1   | 26                  | 4.54             | 2.56   | 21.2     | 10.4–35.8           | 0.17       | 0.85    | 0.71    |
| Makap'u          | 21.293     | 157.536     | 400–442         | 17 | 125 | 2   | 17                  | 4.53             | 2.52   | 66.8     | 0.1–335.1           | 0.09       | 0.82    | 0.77    |
| NW Laysan Island | 25.867     | 171.966     | 494–577         | 30 | 162 | 3   | 30                  | 4.46             | 2.62   | 63.2     | 0.1–317.5           | 0.08       | 0.84    | 0.79    |
| Pioneer Bank     | 25.810     | 173.454     | 476–581         | 18 | 134 | 3   | 18                  | 4.44             | 2.67   | $\infty$ | $\infty$ – $\infty$ | 0.15       | 0.85    | 0.75    |
| Pohue Bay        | 19.001     | 155.814     | 420–525         | 11 | 99  | 4   | 11                  | 4.50             | 2.46   | $\infty$ | $\infty$ – $\infty$ | 0.17       | 0.84    | 0.73    |
| Raita Bank       | 25.639     | 169.318     | 510–562         | 17 | 120 | 2   | 17                  | 4.46             | 2.51   | $\infty$ | $\infty$ – $\infty$ | 0.09       | 0.85    | 0.79    |
| Twin Banks       | 23.264     | 163.998     | 446–459         | 3  | 35  | 0   | 3                   | 3.30             | 1.84   | $\infty$ | $\infty$ – $\infty$ | 0.14       | 0.71    | 0.76    |
| West Northampton | 25.383     | 172.404     | 480–538         | 15 | 110 | 6   | 14                  | 4.27             | 2.37   | 69.7     | 0.1–350             | 0.07       | 0.80    | 0.77    |

<sup>a</sup>Multilocus genotypes at this location do not equal N because one individual was removed from analyses as an outlier  
Metrics with \*were calculated without null allele loci. N Number of Samples, NPA Number of Private Alleles,  $N_e$  Effective population size,  $H_e$  Expected Heterozygosity,  $H_o$  Observed Heterozygosity

the exceptions of Keahole and Makapu'u Points. However, this species primarily occurs at these sites below the maximum harvest depth (~400 m) and a comparison of the size frequency distribution of individuals in Keahole and Makapu'u (Baco et al. 2023) indicated that the coral size distributions of the collected samples were similar to unharvested beds. Therefore, these sites were retained.

It is possible temporal genetic change may have happened over the ~20 years of sampling for this study (1998–2017). However, as noted in the Introduction, coralliids are long lived species (>100 years) and very slow growing. It is also very rare to observe locations with new recruitment of this species (ARB pers. obs.). Thus, there are probably very few specimens that were sampled that recruited during the time frame of this study for these sites. Additionally, as most collections within a single seamount happened within a span of 1–2 years, if any change happened in the long sampling period, it would primarily affect comparisons of samples between seamounts.

## Microsatellite preparation

Small fragments of each colony were collected using the submersible manipulator arm and placed in individual numbered jars in an insulated biobox to prevent contamination between samples. Pieces were also taken from colonies that were sampled whole for other research projects. Sample sizes were generally comparable between populations (15–20 individuals) though Ka'ena Point and Twin Banks had fewer than ten samples (Table 1). Fragments were either cryogenically preserved at –80 °C or in 100% non-denatured ethanol. Coral polyps were dissected from the colony and DNA extraction from 270 individuals was carried out using a Qiagen DNeasy Blood and Tissue DNA Extraction Kit. Modifications to the prescribed method included overnight lysis with proteinase K and a reduction of the recommended final elution buffer volume to 150 µL (instead of 200 µL) was used to increase final DNA concentrations.

Nine total loci were amplified for all samples, five previously described (A2, B1, C2, C12, and O3) (Baco et al. 2006) and four were newly developed (Table 2). To develop new microsatellite loci, genomic libraries from two *H. laauense* individuals were constructed following protocols in the New England Biolabs Illumina Library Prep Kit and sequenced using the Rapid Run paired end method on an Illumina HiSeq 2500. Raw reads were then analyzed for microsatellite sequences of at least six dinucleotide or trinucleotide repeats using the PAL finder program (Castoe et al. 2012). 54 primer pairs were screened as possible candidates, and out of those four new loci (N14, N27, N44, and N54) were obtained.

PCR amplifications for each locus for a 25 µL final volume included 50 ng of DNA, 1X Promega GoTaq PCR

Buffer, 1 mM dNTPs, 1 mM of each primer, and 1.5 U Promega GoTaq polymerase. Forward primers were labeled with HEX fluorescent dye. PCR protocols for each primer pair are available in Table 2. PCR products were sent to the University of Florida Interdisciplinary Center for Biotechnology Research for genotyping using an Agilent 3730 Analyzer with ROX 500 ladder.

## Microsatellite analysis

Fragment length was analyzed using the R package 'Fragman' with default scoring settings for peak calls (Covarrubias-Pazaran et al. 2016) in R version 3.5.2 (R Core Team 2018). All calls were then checked by eye for stutter peaks or amplification of more than two alleles. Null allele frequencies, genotyping error, linkage disequilibrium, and number of migrants were analyzed using Genepop 4.2 online (Raymond and Rousset 1995; Rousset 2008).

To test the ability of these loci to find population differentiation, a power analysis was run. First, effective population size ( $N_e$ ) was estimated using the molecular coancestry method from NeEstimator v2 (Do et al. 2014). This method was used as it is less biased by population substructure, age structure, or small sample sizes (Luikart et al. 2010). The first two are unknown for this species and some locations have relatively small sample sizes (<20 individuals). The power analysis was run using POWSIM v4.1 (Ryman and Palm 2006) with an  $N_e$  of 60, based on results from NeEstimator, and 1000 replications.

Summary statistics for populations and loci were calculated using the R packages 'adegenet' (Jombart 2008), 'PopGenReport' (Adamack and Gruber 2014), and the 'ShannonGen' function (Zahl 1977; Konopiński 2020). Tests for per-locus, per-population Hardy–Weinberg Equilibrium (HWE) were run using 'pegas' (Paradis 2010). Population pairwise  $G'_{ST}$  values and per-locus  $G'_{ST}$  values were calculated with 'mmod' (Winter 2012).  $G'_{ST}$  is preferable to  $F_{ST}$  values for highly variable loci as  $F_{ST}$  is unlikely to ever reach its maximum value of 1.0 for more than two alleles with high heterozygosity, while  $G'_{ST}$  is standardized by the maximal heterozygosity of the locus (Hedrick 2005), which allows  $G'_{ST}$  to reach 1.0 in differentiated populations.

Population differentiation by locations was analyzed using Analysis of Molecular Variance (AMOVA) in the package 'poppr' (Kamvar et al. 2014). Clusters were assigned using *find.cluster* from 'adegenet' based on the BIC criterion and using the Ward method. Discriminant analysis (DAPC) and admixture were analyzed in 'adegenet' both by site and by cluster. These methods are better suited than STRUCTURE for this dataset as they are not affected by deviations from Hardy–Weinberg equilibrium or by linkage disequilibrium (Jombart et al. 2010). IBD was calculated through mantel

**Table 2** Per Locus primers, PCR conditions, and summary statistics

| Locus | Forward primer sequences (5'-3') | Reverse primer sequences (5'-3') | Motif  | Temp (°C)          | No. cycles        | Anneal time (s) | Size Range | No. of alleles | $H_o$ | $H_e$ | $G^*_{ST}$ |
|-------|----------------------------------|----------------------------------|--|--------------------|-------------------|-----------------|------------|----------------|-------|-------|------------|
| B1    | CAGTGACAAATGTTGTA CGAT           | AGCGTGGGGTAAATTGA TA             | (CA)22   | 48                 | 35                | 45              | 142–226    | 32             | 0.84  | 0.97  | 0.382      |
| C12   | CTTCTGGCTCGTTATCGA               | AAGGCTTTCACTTATAAA TAGTCTG       | (CA)21   | 46/43 <sup>a</sup> | 3/35 <sup>a</sup> | 45              | 75–181     | 53             | 0.63  | 0.96  | NA         |
| O3    | GCTTGACCCAAATCAAGTC              | AACGGCTCCCTGGAAAGAAC             | (CAT)18(CGT) (CAT)7                                | 52                 | 35                | 45              | 160–217    | 29             | 0.65  | 0.85  | 0.132      |
| C2    | CGGGTACGCCAGAGTTAAC              | CCAAAACACATGGGATA ACAA           | (CA)20(TA)(CA)3 (TA)(CA)11                         | 48                 | 35                | 45              | 186–251    | 55             | 0.81  | 0.95  | 0.418      |
| A2    | TGAACCCACCAATTAGAA CGA           | AAATTCTAACACGGCCAAT              | (CAGA)3(CA)5(CG) (CA)9(CG)(CA)5 (CG)2(CA)(CG)(CA)8 | 61/58 <sup>a</sup> | 3/25 <sup>a</sup> | 45              | 184–287    | 74             | 0.92  | 0.98  | 0.375      |
| N27   | TGTTATAGTAGCACCCTT CTCGG         | TTCTGACATGAGAACAC TATTGCC        | TC(14)   | 48                 | 35                | 45              | 139–161    | 18             | 0.71  | 0.86  | 0.192      |
| N14   | CCAGTTAATTACACCAAG TGTGCC        | GCTCCGCTAGAAAAGCCG               | AT(14)   | 50                 | 35                | 30              | 165–200    | 21             | 0.46  | 0.85  | NA         |
| N54   | AGGGCTTTGTAATGTTT TGAGGC         | AAAGGATCTAACCGTCC CC             | AT(12)   | 54                 | 35                | 45              | 104–130    | 14             | 0.69  | 0.83  | 0.185      |
| N44   | AAACATACGACGGTGATA ATTCTGG       | CCAACCACAAATGGTCT ATGCG          | AT(12)   | 42                 | 40                | 60              | 192–243    | 18             | 0.76  | 0.68  | 0.044      |

 $H_o$  Observed heterozygosity,  $H_e$  Expected heterozygosity<sup>a</sup>Two-stage PCR conditions with three cycles at first temperature and then 35 or 25 cycles at the second temperature

tests in ‘adegenet’ and linear regressions from the R ‘stats’ package.

Finally, migration models were analyzed using MIGRATE v. 4.4.4 with constant mutation rate, a Brownian motion stepwise mutation model, estimated migration rates between sites, and 5,000,000 Markov chain steps with a burn in of 100,000 steps. The population structures tested in

18 different models can be seen in Table 3, which included models based on predicted connectivity breaks from Toonen et al. (2011) and Selkoe et al. (2014) as well as a single population model and a 16-population model. The best migration model was chosen using the Bayes Factor comparison of the thermodynamic integration likelihood (Beerli 2006; Beerli and Palczewski 2010).

**Table 3** Results of migration models analyzed using MIGRATE

| Model                        | Log(mL)     | LBF         | Rank | Locations in population                                      | Migration model   |
|------------------------------|-------------|-------------|------|--|---|
| 1pop                         | −277,556.39 | −234,081.20 | 19   | All  | All sites are one population  |
| 3pop east to west plus       | −139,731.81 | −96,256.62  | 18   | Breaks in between Raita Bank and Twin Banks                  | All populations send larvae to the west                               |
| 3pop west to east circle     | −137,117.32 | −93,642.13  | 17   |  | Migrants move in a stepping stone from west to east, then circle back |
| 3pop east to west            | −134,611.38 | −91,136.19  | 16   |  | Migrants move between adjacent populations from east to west          |
| 3pop west to east plus       | −132,988.21 | −89,513.02  | 15   |  | All populations send larvae to the east                               |
| 3pop west to east            | −132,456.43 | −88,981.24  | 14   |  | Migrants move between adjacent populations from west to east          |
| 3pop east to west circle     | −131,517.23 | −88,042.04  | 13   |  | Migrants move in a stepping stone from east to west, then circle back |
| 3pop two-way stepping stone  | −125,702.35 | −82,227.16  | 12   |  | Migrants move between adjacent populations in either direction        |
| 3pop all-ways                | −123,466.22 | −79,991.03  | 11   |  | All populations have migration between each other                     |
| 5pop east to west            | −116,158.20 | −72,683.01  | 10   | Breaks at Raita Bank, Twin Banks, Kaua'i, and Makapu'u Point | Migrants move between adjacent populations from east to west          |
| 5pop west to east            | −112,787.97 | −69,312.78  | 9    |  | Migrants move between adjacent populations from west to east          |
| 5pop two-way stepping stone  | −108,467.49 | −64,992.30  | 8    |  | Migrants move between adjacent populations in either direction        |
| 5pop all-ways                | −103,998.82 | −60,523.63  | 7    |  | All populations have migration between each other                     |
| 16pop west to east           | −47,687.87  | −4212.68    | 6    | Each seamount is one population                              | Migrants move between adjacent populations from west to east          |
| 16pop east to west           | −47,414.74  | −3939.55    | 5    |  | Migrants move between adjacent populations from east to west          |
| 16pop west to east circle    | −44,223.31  | −748.12     | 4    |  | Migrants move in a stepping stone from west to east, then circle back |
| 16pop all-ways               | −43,682.59  | −207.40     | 3    |  | All populations have migration between each other                     |
| 16pop east to west circle    | −43,654.65  | −179.46     | 2    |  | Migrants move in a stepping stone from east to west, then circle back |
| 16pop two-way stepping stone | −43,475.19  | 0.00        | 1    |  | Migrants move between adjacent populations in either direction        |

LBF Log Bayes Factor

## Results

### Summary statistics and locus evaluation

All nine loci were highly variable with 14–74 alleles per locus (Table 2). Observed heterozygosity ( $H_o$ ) ranged from 0.69 to 0.92, which was much lower than expected heterozygosity ( $H_e$ ) (0.68–0.98) for all loci except N44 (Table 2). Allelic richness by site and Zahl's estimated diversity were both high for all locations, including those with low sample sizes (Table 1). Genotypic diversity was also high between all individuals as no multilocus genotype was shared between any corals, indicating no asexual reproduction and no clonal individuals within *H. laauense* were sampled at any site on these seamounts (Table 1). Most locations had private alleles except for Brooks Banks NW and Twin Banks, but overall, few private alleles were found for any location, with a maximum of 6 at each of East and West Northhampton (Table 1). Estimated  $N_e$  values were variable between sites: five locations had an infinite population size, four had an  $N_e$  near 65, five sites were near 20, and Ka'ena Pt. and Brooks Banks NW had an estimated  $N_e$  of 6.9 and 10, respectively (Table 1).

Null allele frequencies above 0.1 were found for most populations for two loci, C12 and N14; thus, those two loci were removed from subsequent analyses (Supplementary Table 1). Linkage disequilibrium results were only significant in three of the sixteen populations and only between B1 and O3, B1 and A2, and A2 and O3; thus, no additional loci were removed (Supplementary Table 2). Power analysis for the final seven loci showed a strong ability to detect population structure at a  $p$ -value  $< 0.05$  ( $\chi^2 = 1.000$ , Fisher's exact test = 1.000).

Global tests showed no locus to be in HWE, which is likely related to the low  $H_o$  compared to  $H_e$  found for most loci (Table 2). When considering each population separately, deviations from HWE were found in most populations for 1–3 loci, but no one locus was out of HWE for most of the populations, and no population deviated from HWE across all loci (Supplementary Fig. 1). Sites did not show as large of a difference between  $H_o$  and  $H_e$  as was seen for individual loci. Brooks Banks NW, Keahole Point, and Pohue Bay had the largest differences of 0.13, 0.14, and 0.11, respectively (Table 1).  $F_{IS}$  values by site were generally low to moderate (range 0.01–0.17) with the highest values also at Brooks Banks NW, Pohue Bay, and Keahole Point (Table 1).

### Genetic structure

The effective number of migrants estimated from private alleles by Genepop was on average 5.17 (range 1.96–7.84).

AMOVA attributed the most genetic variation to within individuals (88.2%), but showed significant genetic differentiation between sites, and showed that variation between individuals within sites was significantly higher than expected (Fig. 2; Tables 2, 3, 4 and 5).

$G'_{ST}$  values indicated moderate but significant population differentiation (Global = 0.166, Range 0.0–0.489,  $p = 0.01$ ), with the greatest differences often occurring in pairwise comparisons between other populations and the Ka'ena Point or Kaua'i populations (0.15–0.49) (Table 4). Twin Banks also had  $G'_{ST}$  values greater than 0.2 in 7 of 15 pairwise comparisons and NW Laysan in 6 pairwise comparisons. Interestingly, for discrete populations within a single seamount,  $G'_{ST}$  values were still moderate to high; between the three Brooks Banks populations the average  $G'_{ST}$  was  $0.139 \pm 0.009$ , between Pohue Bay and Keahole Point on the Island of Hawai'i  $G'_{ST}$  was 0.116, and between Makapu'u Point and Ka'ena Point on the Island of O'ahu  $G'_{ST}$  was 0.223.

The visual representation of all populations by site using DAPC showed Ka'ena Point to be a strong outlier from all other populations (Supplementary Fig. 2). This could be due to extreme inbreeding but could also suggest a cryptic species was sampled within that location. After removing that population, DAPC showed overlap between many locations with a horseshoe pattern to the distribution of populations (Fig. 3). A general clustering of the MHI can be seen in the upper left of the ordination; however, Bank 8 and Twin Banks from the NWHI also fall into this cluster rather than with the other NWHI. The remaining NWHI locations comprise the lower ordination sectors, with East and West Northhampton forming a sub-cluster at the tail end of the horseshoe.

Admixture charts for a 16-population model (Fig. 4A) showed that most individuals had a larger probability of belonging to their own population than to any other. Interestingly, this is still true for populations within sites on a single seamount, as individuals from the southeast and southwest sides of Brooks Banks showed little admixture; while, individuals from the northwest side showed highest levels of admixture with Bank 8 rather than the other two sides of Brooks Banks. On the Island of Hawai'i, Keahole Point also showed much less admixture than expected with Pohue Bay, while Pohue Bay showed similar levels of admixture with Keahole Point and Kaua'i (Fig. 4B). Similarly, Makapu'u and Ka'ena on the Island of O'ahu did not show any admixture.

The lowest BIC for k-means clustering, indicated an optimum of five clusters. These clusters did not show a clear geographic pattern. The DAPC scatterplot (Supplementary Fig. 3) shows clusters one and two to be most similar to each other, and clusters three and five group together, while cluster 4 appears to be the most different. The admixture chart

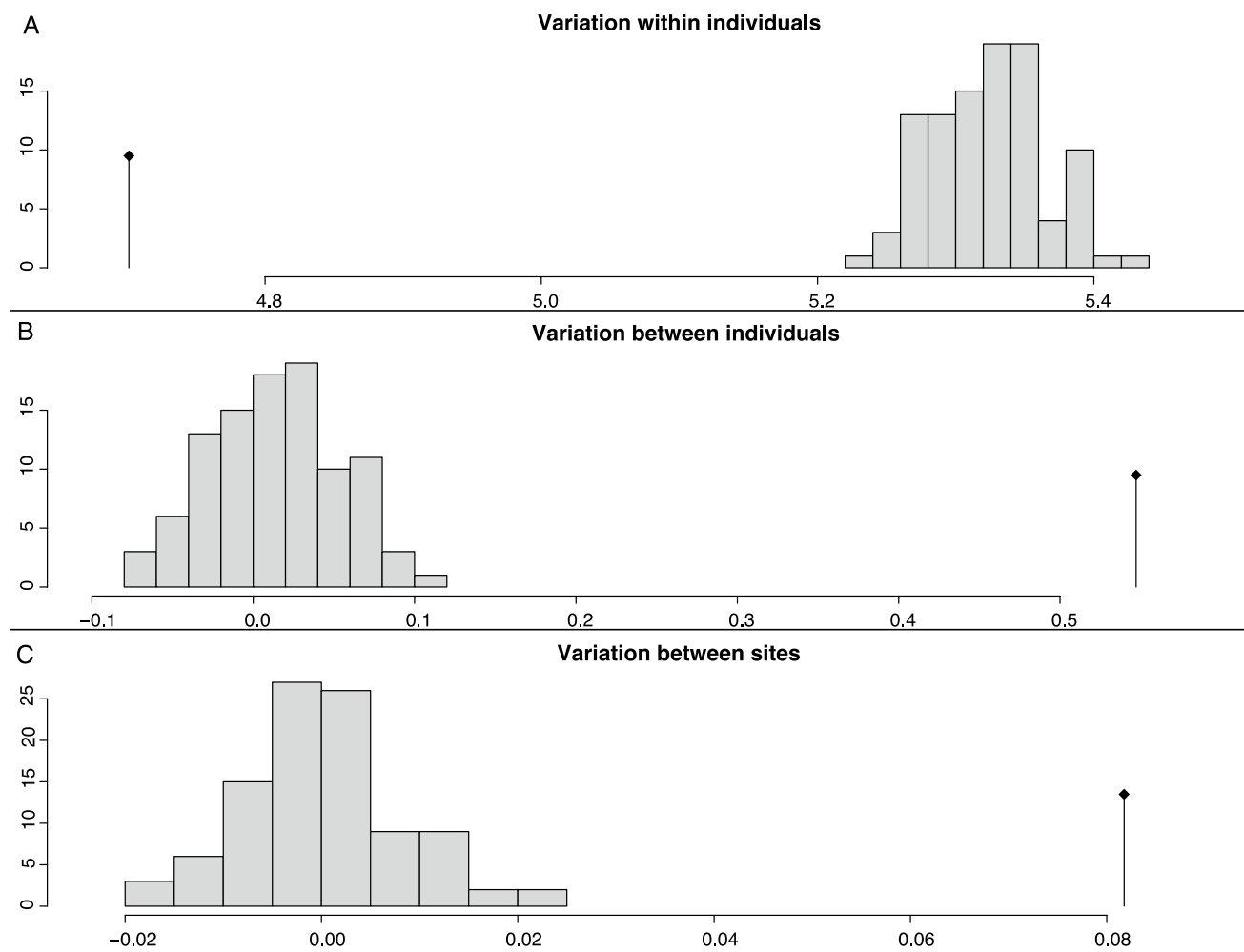


**Fig. 2** Histograms of expected distribution of variance from AMOVA analysis. Measured variance is shown as a black diamond with a line and is significantly different from expected when it falls outside of the histogram

(Supplementary Fig. 4A) shows all clusters can be found at most locations except for Northwest Laysan Island, Kaua'i, and Pohue Bay, Twin Banks, and Ka'ena Pt (Supplementary Fig. 4B). Further discussion on k-means clustering results can be found in the supplementary material.

Though the site-based DAPC shows a slight geographic trend (Fig. 3), tests for patterns of IBD showed mixed results (Fig. 4). The Mantel test and linear regression showed no evidence of IBD ( $R^2 = -0.005, p = 0.28$ ) (Fig. 5A, B). Mantel tests and linear regression were conducted to look for isolation by depth as well, but no evidence was seen for genetic structuring by depth ( $R^2 = -0.055, p = 0.54$ ) (Fig. 5C, D).

Of the 18 migration models tested using MIGRATE, the models with 16 population were the strongest models. In contrast to the Mantel test results, among the MIGRATE models, the one with gene flow moving in a two-way stepping-stone pattern between each adjacent seamount had the best likelihood value. (Table 3; Fig. 6, Supplementary Table 1). Migration rates between features were generally

even and low to moderate ( $M = 0.55\text{--}2.26$ ) while the mutation-scaled effective population size varied widely between locations ( $\Theta = 2.85\text{--}41.78$ ).

## Discussion

### Genetic diversity

This study provides new insights into the genetic diversity and population connectivity of the precious Red Coral *Hemicorallium laauense* throughout a broad expanse of the Hawaiian Archipelago. Data from 7 microsatellite loci from 16 locations indicated very high allelic richness that was comparable across the Archipelago, even for the sites with low sample sizes. *H. laauense* has very high allelic diversity (14–74 alleles per locus) compared to other mesophotic and deep-sea octocoral species. For example, *Funiculina quadrangularis* had 3–40 alleles per locus (Wright et al. 2015),

**Table 4** Pairwise  $G_{ST}$  values across 16 populations

| Site  | B8   | Pio  | WN   | EN   | NWL  | Raita | BBNW | BBSE | BBSW | TB   | Kauai | Kaena | MK   | KP   | PB   |
|-------|------|------|------|------|------|-------|------|------|------|------|-------|-------|------|------|------|
| Pio   | 0.05 |      |      |      |      |       |      |      |      |      |       |       |      |      |      |
| WN    | 0.07 | 0.08 |      |      |      |       |      |      |      |      |       |       |      |      |      |
| EN    | 0.11 | 0.05 | 0.01 |      |      |       |      |      |      |      |       |       |      |      |      |
| NWL   | 0.14 | 0.11 | 0.20 | 0.09 |      |       |      |      |      |      |       |       |      |      |      |
| Raita | 0.01 | 0.08 | 0.06 | 0.10 | 0.12 |       |      |      |      |      |       |       |      |      |      |
| BBNW  | 0.03 | 0.15 | 0.15 | 0.20 | 0.27 | 0.14  |      |      |      |      |       |       |      |      |      |
| BBSE  | 0.02 | 0.13 | 0.13 | 0.15 | 0.10 | 0.09  | 0.15 |      |      |      |       |       |      |      |      |
| BBSW  | 0.11 | 0.05 | 0.19 | 0.20 | 0.19 | 0.14  | 0.15 | 0.13 |      |      |       |       |      |      |      |
| TB    | 0.00 | 0.13 | 0.28 | 0.22 | 0.20 | 0.13  | 0.01 | 0.15 | 0.21 |      |       |       |      |      |      |
| Kauai | 0.28 | 0.34 | 0.34 | 0.28 | 0.20 | 0.23  | 0.41 | 0.28 | 0.46 | 0.31 |       |       |      |      |      |
| Kaena | 0.30 | 0.36 | 0.36 | 0.26 | 0.20 | 0.24  | 0.49 | 0.21 | 0.38 | 0.28 | 0.23  |       |      |      |      |
| MK    | 0.01 | 0.16 | 0.12 | 0.15 | 0.20 | 0.08  | 0.17 | 0.06 | 0.18 | 0.10 | 0.15  | 0.22  |      |      |      |
| KP    | 0.01 | 0.06 | 0.17 | 0.19 | 0.18 | 0.10  | 0.09 | 0.13 | 0.06 | 0.10 | 0.32  | 0.36  | 0.11 |      |      |
| PB    | 0.08 | 0.15 | 0.17 | 0.14 | 0.04 | 0.13  | 0.16 | 0.13 | 0.14 | 0.21 | 0.16  | 0.28  | 0.10 | 0.12 |      |
| CS    | 0.06 | 0.09 | 0.15 | 0.14 | 0.17 | 0.12  | 0.13 | 0.06 | 0.11 | 0.12 | 0.24  | 0.27  | 0.04 | 0.09 | 0.14 |

B8 Bank 8, Pio Pioneer Bank, WN West Northampton, EN East Northampton, NWL Northwest Laysan, BBNW Brooks Banks Northwest, BBSE Brooks Banks Southeast, BBSW Brooks Banks Southwest, TB Twin Banks, MK Mapapu'u, KP Keahole Pointe, and PB Pohue Bay

**Table 5** AMOVA results

| Sample type                            | Df    | Sum of squares | Mean of squares |
|--|-------|----------------|-----------------|
| Between site                           | 15    | 127.91         | 8.53            |
| Between samples within site            | 254   | 1472.08        | 5.80            |
| Within samples                         | 270   | 1269.38        | 4.70            |
| Total                                  | 539   | 2869.38        | 5.32            |
| Components of covariance               | Sigma | %              | P-value         |
| Variations between site                | 0.08  | 1.53           | 0.01            |
| Variations between samples within site | 0.55  | 10.26          | 0.01            |
| Variations within samples              | 4.70  | 88.20          | 0.01            |
| Total variations                       | 5.33  | 100.00         |                 |
| Phi stats                              | Value |                |                 |
| Phi-samples-total                      | 0.12  |                |                 |
| Phi-samples-site                       | 0.10  |                |                 |
| Phi-site-total                         | 0.02  |                |                 |

*Callogorgia delta* and *C. americana* had 3–22 alleles per locus (Quattrini et al. 2015), and *Narella versluysi* had 5–24 alleles per locus (Yesson et al. 2018). High genetic diversity may be a common character of the coralliids, as populations within *C. rubrum* showed similar levels of allelic diversity (7–67 alleles per locus) (Ledoux et al. 2010). High allelic diversity also led to a higher average  $H_e$  (0.68–0.98) in *H. laauense* compared to most other octocoral species (*Eunicella verrucosa*: 0.367–0.459 and *Alcyonium digitatum*: 0.594–0.668 (Holland et al. 2017), and *Eunicella singularis*: 0.28–0.57 (Costantini and Abbiati 2016)), except for *C. rubrum* (0.62–0.82) (Ledoux et al. 2010) and *Paramuricea*

*clavata* (0.56–0.81) (Mokhtar-Jamaï et al. 2011). The high number of alleles could suggest a higher mutation rate for *H. laauense* than typically seen in deep-sea corals, or a large population size that provides exceptionally high genetic diversity (Hague and Routman 2016). However, large population sizes are not supported by NeEstimator results for most populations (Table 1). With *H. laauense* being long lived but slow growing, and possibly continuous spawners, there are likely many overlapping generations of corals within any seamount population that are difficult to tell apart by size alone. Long life spans and multiple generations within a population may allow for high genetic diversity

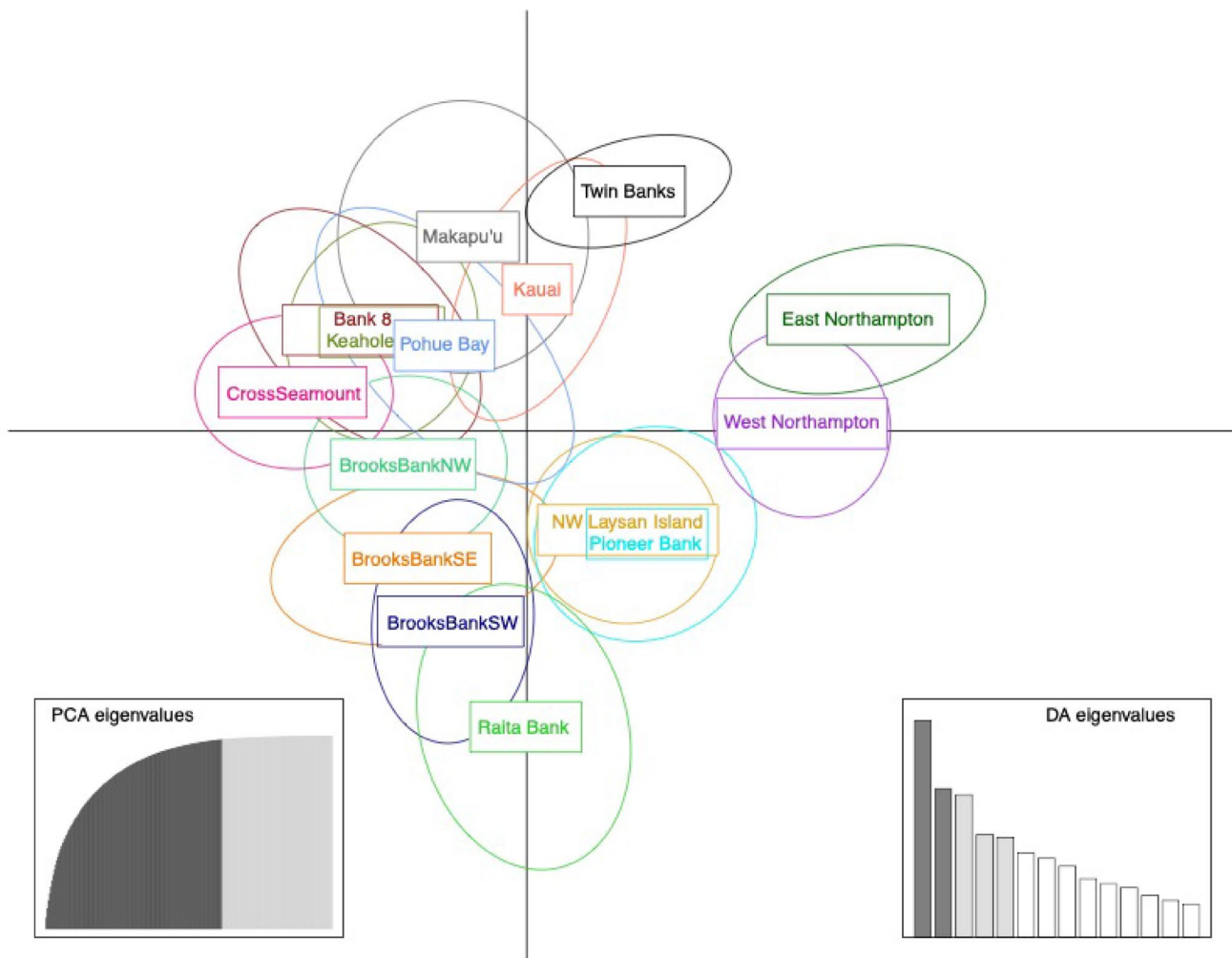


**Fig. 3** DAPC plot of sites after Ka'ena Point is removed as an outlier. Names are placed at the centroid of the sample distribution and ovals show 95% confidence interval

(Ellner and Hairston 1994; Lippe et al. 2006), and longevity could also allow for greater accumulation of neutral mutations, which would also increase allelic diversity (Klekowsky and Godfrey 1989).

$H_e$  was generally higher than  $H_o$  for most sites, with the largest differences at Brooks Banks NW, Pohue Bay, and Keahole Point. Pohue Bay and Keahole Point also showed higher  $F_{IS}$  values ( $F_{IS}=0.17$ ). Brooks Banks NW shows the second highest level of heterozygote deficiency and had the highest  $F_{IS}$  value ( $F_{IS}=0.20$ ). The two other Brooks Banks locations also have moderate  $F_{IS}$  values ( $F_{IS}=0.13$ ), thus, populations within this seamount may have a higher level of self-recruitment than other locations. Higher  $F_{IS}$  values at both locations on the Island of Hawai'i may also indicate higher levels of inbreeding. High  $F_{IS}$  values combined with higher  $G'_{ST}$  values among sites within a single seamount suggest a lack of external sources for propagules for each population, even from within the same seamount, which

may lead to inbreeding. The alternative that high  $F_{IS}$  values at these locations would be due to the Wahlund effect, of combining data from different populations (Wahlund 1928), seems unlikely as most samples were collected from a relatively small area. The exception is the high  $F_{IS}$  value at Pioneer, which may indicate further population structuring within the site. Two groups of samples from this site are separated by ~ 1 km, but one group only included 4 individuals which precluded separating samples into 2 populations for analyses. The range of  $F_{IS}$  values found in *H. laauense* are similar to a preliminary study based on three loci (Baco and Shank 2005) and to other octocorals showing low to moderate inbreeding including *Eunicella verrucosa* ( $F_{IS}=-0.20$  to 0.14) (Holland et al. 2017) and *Paramuricea clavata* ( $F_{IS}=-0.02$  to 0.10) (Pérez-Portela et al. 2016) and slightly lower than values for *C. rubrum* ( $F_{IS}=0.20$ –0.47), which has high local recruitment.  $F_{IS}$  values for octocorals showing almost no inbreeding are generally much lower

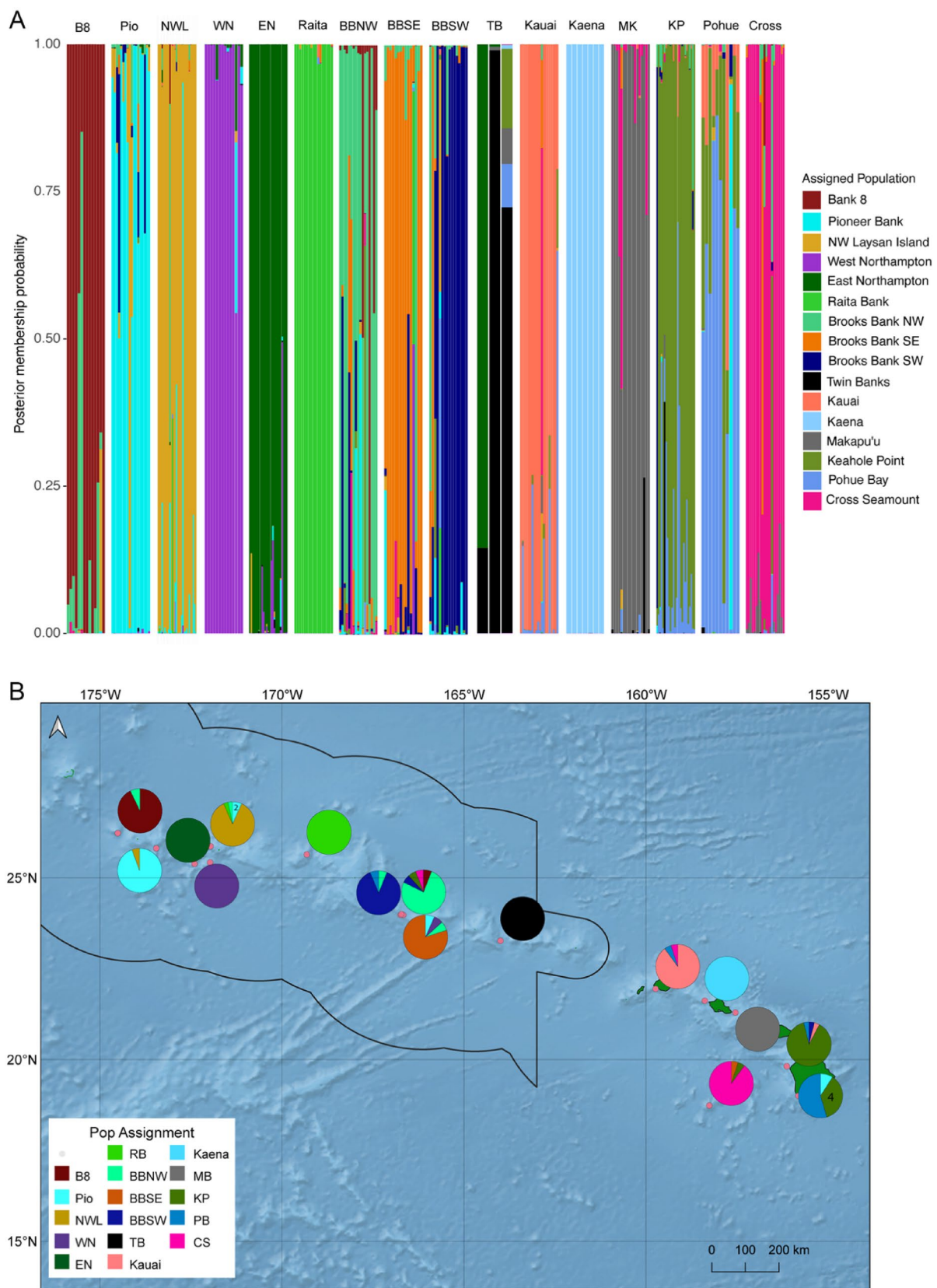


**Fig. 4** **A** Admixture chart by site showing the site each sample most likely originated from. **B** Pie charts showing population assignment of samples compared to location of collection. Minority wedges with-

out numbers show one individual assigned to a population other than the one it was collected from

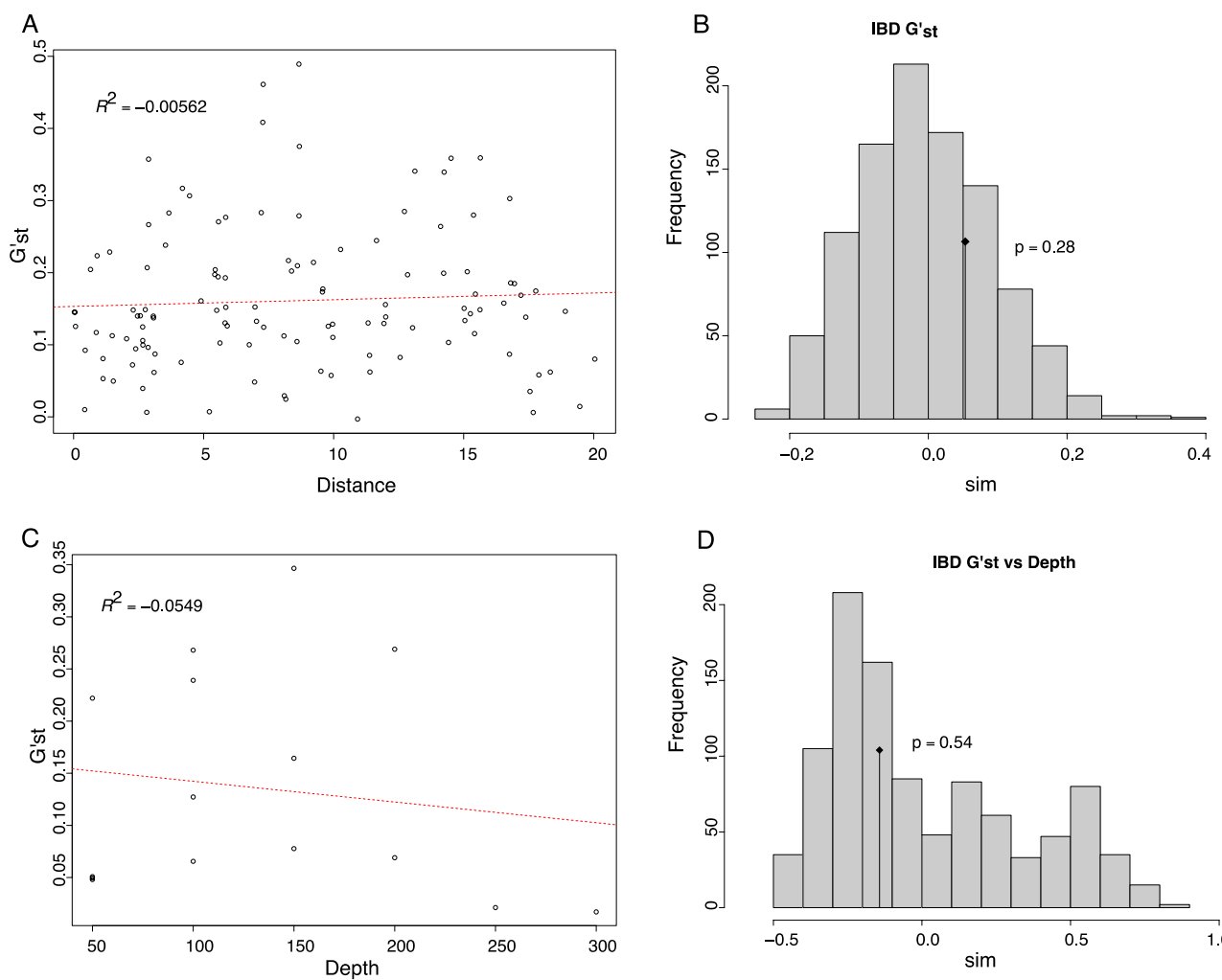


**Fig. 5** Results of Mantels tests for isolation by distance and depth. **A** Scatter plot of  $G^{'}_{ST}$  genetic distance versus geographic distance. **B** Histogram of random tests for correlations between  $G^{'}_{ST}$  and distances with the original value shown by the black diamond. **C** Scatter

plot of  $G^{'}_{ST}$  genetic distance versus pairwise depth differences among populations split into depth bins every 50 m. **D** Histogram of random tests for correlations between  $G^{'}_{ST}$  and depth bins with the original value shown by the black diamond

(*Funiculina quadrangularis* ( $F_{IS} = -0.004$  to  $0.045$ ) (Wright et al. 2015) and *Alcyonium digitatum* ( $F_{IS} = -0.001$  to  $0.068$ ) (Holland et al. 2017)).

### Genetic structuring within a seamount

Multiple discrete populations were sampled on different sides for each of three seamounts: Hawai'i, O'ahu, and Brooks Banks. Pairwise  $G^{'}_{ST}$  values for the different populations within each feature were similar to the global  $G^{'}_{ST}$  and at the higher end of the range of pairwise values. The pairwise comparison of Ka'ena Point to Makapu'u Point on O'ahu (113 km distance), had the highest for within feature  $G^{'}_{ST}$  comparisons ( $G^{'}_{ST} = 0.22$ ). The structure between these populations is possibly enhanced by the likelihood of a cryptic species at Ka'ena Point as shown

in DAPC and admixture results (Fig. 4A, Supplementary Fig. 2). While Ka'ena individuals are all assigned to their own population, Makapu'u has some with mixed assignments to nearby Cross Seamount (Fig. 4B). Bottom currents at some locations could have a strong effect on the larval dispersal distances for this species. Makapu'u Point was dominated by a moderate (13.6 cm/s) north–south flow over the course of a year (Parrish and Oliver 2020), which could be limiting gene flow to this location, making local recruitment more likely. Unless larvae are further advected to the east or west during dispersal, they would be pushed off the seamount into much deeper water. Parrish and Oliver (2020) also suggested that Makapu'u Point was not an optimal settling location for *H. laauense* because another coralliid species, *P. secundum*, is far more abundant at this site. *P. secundum* may be able to better

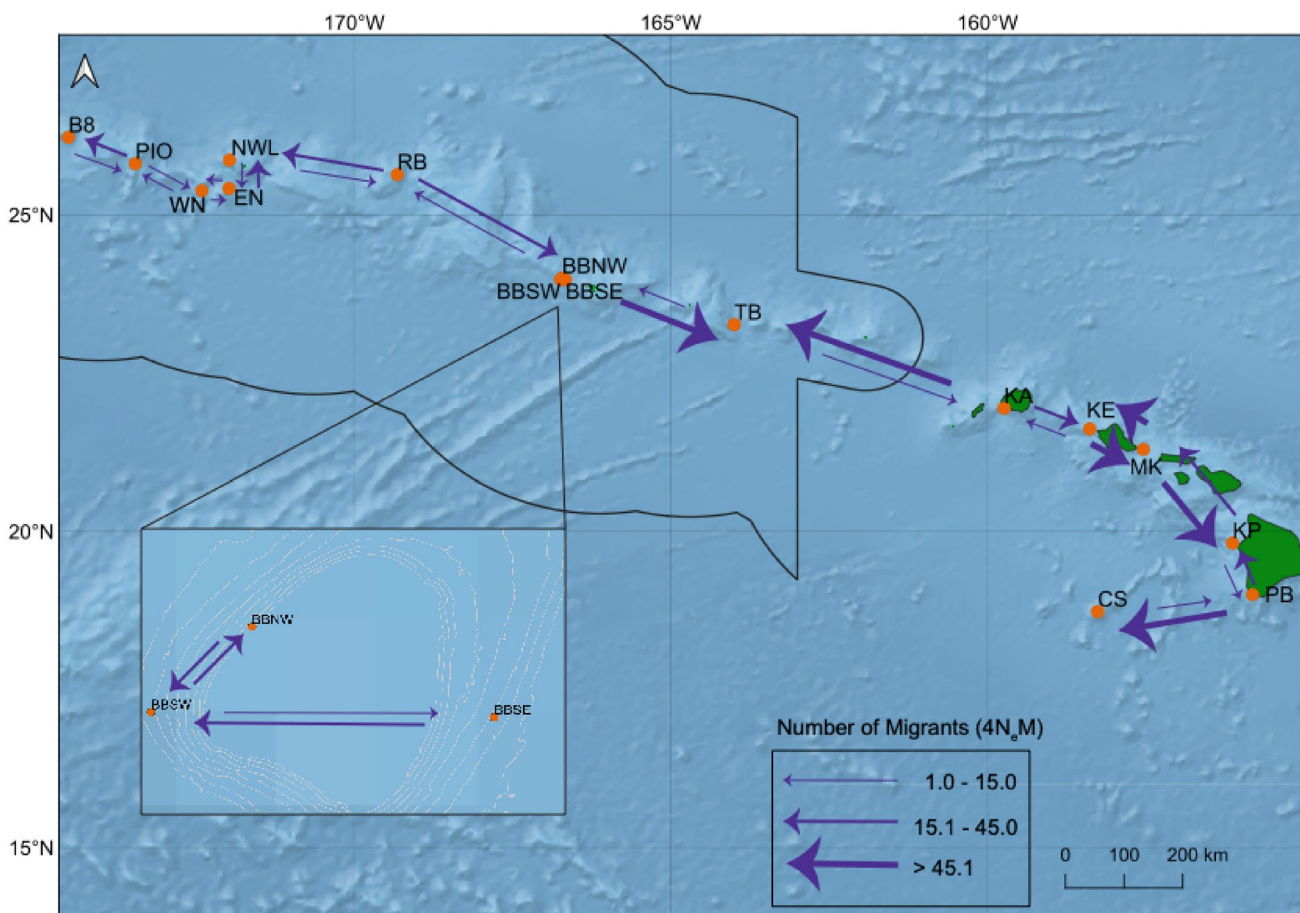


**Fig. 6** Depiction of direction and scale of estimated migrations from the two-way stepping-stone model determined by MIGRATE. *B8* Bank 8, *Pio* Pioneer Bank, *WN* West Northampton, *EN* East North-

ampton, *NWL* Northwest Laysan, *BBNW* Brooks Banks Northwest, *BBSE* Brooks Banks Southeast, *BBSW* Brooks Banks Southwest, *TB* Twin Banks, *MK* Mapapu'u, *KP* Keahole Pointe, and *PB* Pohue Bay

handle stronger currents due to its more robust branching morphology. *H. laauense* also has different preferences for slope and bottom relief (Parrish 2007). If Makapu'u Point is a marginal habitat for *H. laauense*, then self-recruitment is more likely to dominate in that area (Holland et al. 2017).

Keahole Point and Pohue Bay in the Island of Hawai'i are separated by 99 km and had a pairwise  $G'_{ST}$  value of 0.12. These two populations cluster quite closely together in the DAPC (Fig. 3) and show moderate admixture between each other (Fig. 4A, B). Keahole Point has also had bottom current measurements and showed low flow (average 4.6 cm/s) with northward pulses (Parrish and Oliver 2020). Low flow could cause larvae to be mostly retained within Keahole Point or trapped between Hawai'i and Maui Islands if they are advected north and off the seamount (Qiu et al. 1997). Four colonies from Pohue Bay were assigned to Keahole Point, which suggests that there is some recruitment towards the south even though the

dominant bottom current at Keahole Point is northward (Fig. 4B).

The structuring between the three populations on Brooks Banks is the most surprising as they are separated by only 3–8 km of distance yet have moderate pairwise  $G'_{ST}$  values ( $G'_{ST} = 0.15, 0.15$ , and  $0.13$ ). The three populations cluster in the same area of the DAPC (Fig. 3), but Brooks Banks NW seems more similar to populations of the MHI while the southern Brooks Banks cluster more closely to Raita Bank of the NWHI. The three populations show some of the highest levels of admixture of any feature (Fig. 4A), especially Brooks Banks NW which has individuals that were assigned to BB SW, Bank 8, Keahole Point, and Cross Seamount (Fig. 4B). Brooks Banks SE and SW each have one coral colony that may have originated from Brooks Banks NW. Brooks Banks is not an emergent feature, but the summit does reach less than 100 m depth, which could act as a barrier to deep-sea larval dispersal among sides. There are also some depth differences among the populations on

Brooks Banks, which could also be limiting larval dispersal between the populations (e.g., Cho and Shank 2010; Miller et al. 2011; Quattrini et al. 2015; Miller and Gunasekera 2017). The depth range of Brooks Banks NW sampling (417–442 m) is non-overlapping with the depth range of Brooks SE (454–462 m) and Brooks SW (448–590 m) (Table 1).

Similarly on Hawai'i, colonies collected from Pohue Bay (420–525 m) were deeper than Keahole Point (385–410 m). Again, the shallower location shows more gene flow than the deeper location, which may indicate that larvae from *H. laauense* are not particularly buoyant, not effective swimmers, or are more gravitactic, similar to *C. rubrum* (Santangelo et al. 2003). Depth may contribute to differentiation among populations; however, Makapu'u Point and Ka'ena Point have fully overlapping depth distributions, and no isolation by depth was found overall for samples from the Archipelago (Fig. 5C, D). Thus, depth does not appear to be a consistent driver of differences between populations over broader scales.

Fine-scale population differences have been seen in other temperate and deep-sea coral species. *H. laauense* showed a significant  $R_{ST}$  value (0.170) between two populations less than 2 km apart on Makapu'u Point (Baco and Shank 2005). *P. clavata* from throughout the Mediterranean has shown genetic differentiation at scales as small as 5 km for populations within canyons (Pérez-Portela et al. 2016) and off islands and continental shelves (Mokhtar-Jamaï et al. 2011). *Callogorgia delta* showed population structure at locations just 15 km apart in the Gulf of Mexico, both when those locations were separated by a large depth difference (189 m) and small depth differences (14 m). Recently, the deep-sea scleractinian *Solenososmilia variabilis* was also found to have significant population structuring within a few hundred meters on two seamounts in the Tasmanian Sea (Miller and Gunasekera 2017). These corals may rely upon asexual reproduction more heavily than most octocoral species, which would contribute to differentiation at such a small scale (Miller and Gunasekera 2017).

## Genetic structuring among seamounts

When comparing genetic structuring between seamounts,  $G'_{ST}$  values indicate low to moderate levels of population differentiation, with a wide range of values in pairwise comparisons ( $G'_{ST}=0.0\text{--}0.489$ ) (Table 3). The results for tests of IBD were inconsistent, with Mantel tests not following a pattern of IBD, but MIGRATE contrastingly showing highest exchange among neighboring populations (Supplemental Table 3; Fig. 6). Results from MIGRATE are also very similar to dispersal models in shallow-water Hawaiian species showing greater dispersal to the northwest overall, but high levels of self-recruitment that would typically lead

to IBD patterns. However, a lack of an IBD pattern in *H. laauense* matches with evidence from other studies in the Archipelago that show IBD is not a dominant structuring mechanism despite the stepping-stone geographic layout of the seamounts (Toonen et al. 2011; Selkoe et al. 2014). Another consideration for IBD patterns might be whether precious corals that have experienced over-harvesting from tangle-net trawling, might have resulted in any seamount populations being lost, which would heavily affect stepping-stone patterns and between-seamount population structuring. This study focused on sites that are expected to have nearly pristine populations, however, with little to no history of trawl harvests; thus, it is unlikely any stepping-stone populations have been lost. The lack of an IBD pattern despite significant genetic differences among most pairwise population comparisons may be tied to the high allelic diversity of this species, or potentially to recruitment processes that cause a sweepstakes effect on reproductive success and can lead to "genetic patchiness" (Hedgecock et al. 2007). This then can lead to a chaotic population structure, typically seen as genetic structure at small scales in populations that show low differentiation at larger scales (Johnson and Black 1982; Hedgecock and Pudovkin 2011). This chaotic pattern of genetic structure at multiple spatial scales is more similar to shallow-water species in the Archipelago (Rivera et al. 2011; Skillings et al. 2011; Conception et al. 2014; Selkoe et al. 2014). Chaotic patterns may be caused by sweepstakes recruitment (Hedgecock et al. 2007) but are also often found when population genetic structure is more strongly tied to aspects of the environment, or seascape, than they are to geographic distance (Selkoe et al. 2008; Iannucci et al. 2020). A seascape analysis of this species may reveal new insights into these processes.

Kaua'i and Ka'ena Point show the strongest differentiation from most other locations, and these features are typically highlighted as areas of breaks in dispersal and connectivity for many marine species along the Hawaiian Archipelago (Treml et al. 2008; Toonen et al. 2011; Selkoe et al. 2014; Wren et al. 2016). Kaua'i has also been highlighted as having very high expected self-recruitment in bio-physical models of connectivity compared to many other features in the Archipelago (Wren et al. 2016). Interestingly, in this study, Kaua'i and Ka'ena Point do not have heterozygote deficiencies, nor do they have high  $F_{IS}$  values, which suggests these locations are not solely self-recruiting. Based on three microsatellite loci, previous work on *H. laauense* showed high  $F_{IS}$  values and heterozygote deficiencies for one locus for corals from Ka'ena Point, but not for other loci nor at Kaua'i for any locus.  $R_{ST}$  values were significant and as high as 0.14 for comparing Kaua'i to several other sites. Fewer comparisons to Ka'ena were significant, but the range was higher (up to 0.21) (Baco and Shank 2005). Combined with Ka'ena Point's outlier position in the DAPC, these

corals are more likely a recently diverged cryptic species of *Hemicorallium* rather than an isolated population. The high variability of allele frequencies within each feature may deflate pairwise  $G'_{ST}$  values (Willis et al. 2017). While  $G'_{ST}$  allows for greater sensitivity in highly heterozygous populations because it is standardized by the maximal heterozygosity (Hedrick 2005), the extreme allelic diversity within populations of *H. laauense* could still make comparisons based on allele frequencies less robust. AMOVA showed the variation within locations was significantly higher than expected (Fig. 2), and that variation within each site could confound tests for genetic structuring between features by increasing noise within the data.

DAPC also suggests a more complicated relationship between populations that implies processes other than simply geographic distance influence the genetic structure of this species. Once the outlier of Ka'ena Point is removed, the ordination plot shows a clear horseshoe pattern with East and West Northampton at one end, and the MHI and Twin Banks at the other (Fig. 3). While discriminant analyses are not known to have a relationship between gradients and horseshoe patterns as PCA and NMDS plots do (Podani and Miklós 2002), this horseshoe pattern was also demonstrated for simulated stepping-stone dispersal data (Jombart et al. 2010) and could support the stepping-stone pattern supported by the MIGRATE model. There does appear to be a smaller-scale geographic trend in differentiation, where closer sites are more similar in the DAPC plot, apart from Bank 8 and Twin Banks of the NWHI clustering within the MHI sites.

For the admixture analysis by site, individuals are typically assigned to their original location (Fig. 4A). Northwest Laysan Island and Brooks Banks NW show the highest level of admixture for the NWHI, while Keahole Point and Pohue Bay show the highest for the MHI. Admixture between other neighboring locations is less than would be expected from the lower  $G'_{ST}$  values. The Northampton locations have very little overlap and Raita Bank also shows little admixture. Interestingly, some locations that have admixture have individuals assigned to more distant populations rather than adjacent ones: Bank 8 shares allele frequencies mostly with Brooks Banks NW, Kaua'i shows admixture with Pohue Bay, and the 3 Brooks Banks locations show little admixture with each other. For most sites, only 2–4 individuals are assigned to a location they were not sampled from (Fig. 4B). Pohue Bay is the only location with five individuals reassigned to a new location, four of those going to nearby Keahole Point.

## Conservation considerations

The life history and habitat role of *H. laauense* make it a VME indicator species, and it should be protected and

conserved according to the resolutions enacted by the United Nations General Assembly (UN General Assembly 2005, 2007, 2010). Populations within the MHI are less protected, and precious coral harvesting is still permitted within Hawaiian waters, though the expensive gear required for selective harvesting of precious corals has halted harvests in this region (Bruckner 2016). The distributional range of *H. laauense* also extends into high seas areas that are still experiencing active trawl fisheries. The designation of precious corals as VME species should provide greater protections to these coral beds from human impacts, including commercial harvests. Loss of individuals within a feature could then cause a sharp loss in local genetic diversity as rare alleles are lost, and the most likely MIGRATE model suggests limited external locations for new propagules as only adjacent features showed migration. Some populations of *H. laauense* may already have inbreeding depression as shown by moderate  $F_{IS}$  and low  $N_e$  values (i.e., Keahole Point and Brooks Banks NW (Table 1)), and these populations would be even more susceptible to further isolation should adjacent populations be reduced.

*Hemicorallium* seems to require consistent environments with low variability in temperature and salinity (Parrish and Oliver 2020). Despite many populations being protected from direct human impacts, climate change could affect these sensitive populations as even deep waters (200–1000 m) continue to warm (Brito-Morales et al. 2020; Morato et al. 2020) with changes at the depth ranges of *Hemicorallium* in the Pacific of up to 3.63 °C (Sweetman et al. 2017). Small thermal differences could limit successful recruitment of *H. laauense* to previously suitable locations. Acidification is also expected to cause changes in ocean pH, including at bathyal depths of 200–3000 m (Sweetman et al. 2017), and could cause increased dissolution of coral skeletons, especially as high-magnesium calcite, the main form of calcium carbonate in Coralliidae (Weinbauer et al. 2000), is more readily dissolved than aragonite (Morse et al. 2006). Acidification could also affect larval transport post spawning (Byrne 2011). Decreases in oxygen are also expected to be greatest between 200 and 700 m depth (Levin and Bris 2015; Sweetman et al. 2017), which is the prime depth range for these corals. While the oxygen tolerance of *Hemicorallium laauense* specifically is not known, other corals have been shown to be sensitive to lower oxygen levels (Vaquer-Sunyer and Duarte 2008).

## Conclusions

*H. laauense* is widely distributed in the Hawaiian Archipelago, but little information is known about the reproductive strategy, fecundity, settlement strategy, or true habitat suitability despite its long history as a fisheries species in

Hawaiian waters. From the microsatellite data used in this study, it appears that most sites have moderate population differentiation, some inbreeding, and low migration between them, but occasional connectivity at long distances suggests a more chaotic population structure caused by episodic recruitment. Low migration rates and overlapping generations could also be limiting genetic drift within each population, masking true population structure, and causing inflated connectivity estimates. While the markers used in this study were shown to have statistical power to find differences in populations, new loci may be required to fully describe population connectivity for *H. laauense* in the Hawaiian Archipelago. Nevertheless, this is an important VME species that should be protected from further direct human impacts so that populations may be resilient enough to handle indirect impacts from climate change and ocean acidification.

## Permits

This work was conducted under permit numbers: SCP 1999-31 and SCP2001-14, within the Papahānaumokuākea Marine National Monument permits: PMNM-2011-037, PMNM-2014-028, PMNM-2016-02, and PMNM-2019-016. Corals collected in the Northwestern Hawaiian Islands in 2003 were collected when it was the NWHI Coral Reef Ecosystem Reserve, prior to the establishment of the PMNM, under permit numbers NWHICRER-2003-003 and NWHICRER-2003-004.

**Supplementary Information** The online version contains supplementary material available at <https://doi.org/10.1007/s00227-023-04282-5>.

**Acknowledgements** We would like to thank the pilots and crew members of the Hawaii Undersea Research Laboratory *Pisces IV* and *Pisces V* submersibles, the crew members of the *R/V Ka'imiakai-O-Kanaloa*, and the volunteers at sea who helped collect samples: Arvind Shantharam, Kelci Miller, Beatriz Mejia Mercado, Allison Metcalf, Kelly Klein, Savannah Goode, Jessie Perelman, Ellen Bartow-Gillies, Danielle Schimenti, Travis Ferguson, Ann Tarrant and T.M. Shaun Johnston. Frank Parrish and Rick Grigg provided a portion of the specimens for this study from their collections on shared cruises.

**Author contributions** All authors have agreed to be listed and approved the submitted version of the manuscript. All authors contributed to the writing of the manuscript and performed laboratory work, ARB designed the research, and NBM performed data analysis. This manuscript is an original work and has not been published and is not under consideration for publication elsewhere. We have no conflicts of interest to disclose.

**Funding** Specimen collections were funded by grants to ARB from HURL grants awarded in 1998 – 2002 and 2011, Hawaii Sea Grant awarded in 2002, OE HI grants NA03OAR4600108, NA03OAR4600110, and NA04OAR460007, and NSF grant numbers OCE-1334652 to ARB and OCE-1334675 to E. Brendan Roark.

**Data availability** Raw fragment length data, compiled fragment length analyses, and associated metadata have been uploaded to the Dryad

data repository and can be found at <https://doi.org/10.5061/dryad.qjq2bqk7>.

## Declarations

**Conflict of interest** The authors have no relevant financial or non-financial interests to disclose.

**Ethics approval** This study did not require an ethics approval.

## References

Adamack AT, Gruber B (2014) PopGenReport: simplifying basic population genetic analyses in R. *Methods Ecol Evol* 5:384–387. <https://doi.org/10.1111/2041-210X.12158>

Andrews AH, Cordes EE, Mahoney MM, Munk K, Coale KH, Caillet GM (2002) Age, growth and radiometric age validation of a deep-sea, habitat-forming gorgonian (*Primnoa resedaeformis*) from the Gulf of Alaska. *Hydrobiologia* 471:101–110

Andrews AH, Stone RP, Lundstrom CC, DeVogelaere AP (2009) Growth rate and age determination of bamboo corals from the northeastern Pacific Ocean using refined 210Pb dating. *Mar Ecol Prog Ser* 397:173–185. <https://doi.org/10.3354/meps08193>

Ardila NE, Giribet G, Sánchez JA (2012) A time-calibrated molecular phylogeny of the precious corals: reconciling discrepancies in the taxonomic classification and insights into their evolutionary history. *BMC Evol Biol* 12:246. <https://doi.org/10.1186/1471-2148-12-246>

Baco AR (2007) Exploration for deep-sea corals on North Pacific seamounts and islands. *Oceanography* 20:108–117. <https://doi.org/10.5670/oceanog.2007.11>

Baco AR, Shank TM (2005) Population genetic structure of the Hawaiian precious coral *Corallium laauense* (Octocorallia: Corallidae) using microsatellites. In: Friewald A, Roberts JM (Eds). Springer, pp 663–678

Baco AR, Clark AM, Shank TM (2006) Six microsatellite loci from the deep-sea coral *Corallium laauense* (Octocorallia: Corallidae) from the islands and seamounts of the Hawaiian Archipelago. *Mol Ecol Notes* 6:147–149. <https://doi.org/10.1111/j.1471-8286.2005.01170.x>

Baco AR, Morgan NB, Roark EB, Silva M, Shamberger KEF, Miller K (2017) Defying dissolution: discovery of deep-sea scleractinian coral reefs in the North Pacific. *Sci Rep*. <https://doi.org/10.1038/s41598-017-05492-w>

Baco AR, Morgan NB, Roark EB, Biede V (2023) Bottom contact fisheries disturbance and signs of recovery of precious corals in the Northwestern Hawaiian Islands and Emperor Seamount Chain. *Ecol Ind* 148:110010. <https://doi.org/10.1016/j.ecolind.2023.110010>

Baillon S, Hamel J-F, Wareham VE, Mercier A (2012) Deep cold-water corals as nurseries for fish larvae. *Front Ecol Environ* 10:351–356. <https://doi.org/10.1890/120022>

Baker KD, Wareham VE, Snelgrove PVR, Haedrich RL, Fifield DA, Edinger EN, Gilkinson KD (2012) Distributional patterns of deep-sea coral assemblages in three submarine canyons off Newfoundland, Canada. *Mar Ecol Prog Ser* 445:235–249. <https://doi.org/10.3354/meps09448>

Beerli P (2006) Comparison of Bayesian and maximum-likelihood inference of population genetic parameters. *Bioinformatics* 22:341–345. <https://doi.org/10.1093/bioinformatics/bti803>

Beerli P, Palczewski M (2010) Unified framework to evaluate panmixia and migration direction among multiple sampling locations. *Genetics* 185:313–326. <https://doi.org/10.1534/genetics.109.112532>

Bell JB, Alt CHS, Jones DOB (2016) Benthic megafauna on steep slopes at the Northern Mid-Atlantic Ridge. *Mar Ecol* 37:1290–1302. <https://doi.org/10.1111/maec.12319>

Bo M, Pusceddu A, Schroeder K, Bavestrello G, Bertolino M, Borghini M, Castellano M, Harriague AC, Di Camillo CG, Gasparini G, Misic C, Povero P (2011) Characteristics of the mesophotic megabenthic assemblages of the Vercelli seamount (North Tyrrhenian Sea). *PLoS One* 6:e16357. <https://doi.org/10.1371/journal.pone.0016357>

Brito-Morales I, Schoeman DS, Molinos JG, Burrows MT, Klein CJ, Arafah-Dalmau N, Kaschner K, Garilao C, Kesner-Reyes K, Richardson AJ (2020) Climate velocity reveals increasing exposure of deep-ocean biodiversity to future warming. *Nat Clim Chang* 10:576–581. <https://doi.org/10.1038/s41558-020-0773-5>

Bruckner AW (2016) Advances in management of precious corals to address unsustainable and destructive harvest techniques. Springer, pp 747–786

Buhl-Mortensen L, Vanreusel A, Gooday AJ, Levin LA, Priede IG, Buhl-Mortensen P, Gheerardyn H, King NJ, Raes M (2009) Biological structures as a source of habitat heterogeneity and biodiversity on the deep ocean margins. *Mar Ecol* 31:21–50. <https://doi.org/10.1111/j.1439-0485.2010.00359.x>

Byrne M (2011) Impact of ocean warming and ocean acidification on marine invertebrate life history stages: Vulnerabilities and potential for persistence in a changing ocean. CRC Press-Taylor & Francis Group, Boca Raton, pp 1–42

Castoe TA, Poole AW, de Koning APJ, Jones KL, Tombak DF, Oyler-McCance SJ, Fike JA, Lance SL, Streicher JW, Smith EN, Pollock DD (2012) Rapid microsatellite identification from illumina paired-end genomic sequencing in two birds and a snake. *PLoS ONE*. <https://doi.org/10.1371/journal.pone.0030953>

CBD (2011) Strategic Plan for Biodiversity 2011–2020 and the Aichi Targets. Convention on Biological Diversity

Cho W, Shank TM (2010) Incongruent patterns of genetic connectivity among four ophiuroid species with differing coral host specificity on North Atlantic seamounts. *Mar Ecol* 31:121–143. <https://doi.org/10.1111/j.1439-0485.2010.00395.x>

Conception GT, Baums IB, Toonen RJ (2014) Regional population structure of *Montipora capitata* across the Hawaiian Archipelago. *Bull Mar Sci* 90:1–20. <https://doi.org/10.5343/bms.2012.1109>

Costantini F, Abbiati M (2016) Into the depth of population genetics: pattern of structuring in mesophotic red coral populations. *Coral Reefs* 35:39–52. <https://doi.org/10.1007/s00338-015-1344-5>

Costantini F, Fauvelot C, Abbiati M (2007) Fine-scale genetic structuring in *Corallium rubrum*: evidence of inbreeding and limited effective larval dispersal. *Mar Ecol Prog Ser* 340:109–119. <https://doi.org/10.3354/meps340109>

Costantini F, Rossi S, Pintus E, Cerrano C, Gili JM, Abbiati M (2011) Low connectivity and declining genetic variability along a depth gradient in *Corallium rubrum* populations. *Coral Reefs* 30:991–1003. <https://doi.org/10.1007/s00338-011-0771-1>

Covarrubias-Pazaran G, Diaz-Garcia L, Schlautman B, Salazar W, Zalapa J (2016) Fragman: an R package for fragment analysis. *BMC Genet* 17:1–8

Do C, Waples RS, Peel D, Macbeth GM, Tillett BJ, Ovenden JR (2014) NeEstimator v2: Re-implementation of software for the estimation of contemporary effective population size (Ne) from genetic data. *Mol Ecol Resour* 14:209–214. <https://doi.org/10.1111/1755-0998.12157>

Ellner S, Hairston NG (1994) Role of overlapping generations in maintaining genetic variation in a fluctuating environment. *Am Nat* 143:403–417

Figueroa DF, Baco AR (2014) Complete mitochondrial genomes elucidate phylogenetic relationships of the deep-sea octocoral Families Coralliidae and Paragorgiidae. *Deep Sea Res Part II* 99:83–91. <https://doi.org/10.1016/j.dsrr.2013.06.001>

Genin A, Dayton PK, Lonsdale PF, Spiess FN (1986) Corals on seamount peaks provide evidence of current acceleration over deep-sea topography. *Nature* 322:59–61. <https://doi.org/10.1038/322059a0>

Genin A, Noble M, Lonsdale PF (1989) Tidal currents and anticyclonic motions on two North Pacific seamounts. *Deep Sea Res Part A Oceanograph Res Papers* 36:1803–1815

Grigg RW (1976) Fishery management of precious and stony corals in Hawaii

Grigg RW (1993) Precious coral fisheries of Hawaii and the US Pacific Islands. *Mar Fish Rev* 55:50–60

Grigg RW (2002) Precious corals in Hawaii: Discovery of a new bed and revised management measures for existing beds. *Mar Fish Rev* 64:13–20

Guinotte JM, Orr J, Cairns S, Freiwald A, Morgan L, George R (2006) Will human-induced changes in seawater chemistry alter the distribution of deep-sea scleractinian corals? *Front Ecol Environ* 4:141–146

Hague MTJ, Routman EJ (2016) Does population size affect genetic diversity? A test with sympatric lizard species. *Heredity* (Edinb) 116:92–98. <https://doi.org/10.1038/hdy.2015.76>

Hedgecock D, Pudovkin AI (2011) Sweepstakes reproductive success in highly fecund marine fish and shellfish: a review and commentary. *Bull Mar Sci* 87:971–1002. <https://doi.org/10.5343/bms.2010.1051>

Hedgecock D, Launey S, Pudovkin AI, Naciri Y, Lapègue S, Bonhomme F (2007) Small effective number of parents (Nb) inferred for a naturally spawned cohort of juvenile European flat oysters *Ostrea edulis*. *Mar Biol* 150:1173–1182. <https://doi.org/10.1007/s00227-006-0441-y>

Hedrick PW (2005) A standardized genetic differentiation measure. *Evolution (n y)* 59:1633–1638. <https://doi.org/10.1111/j.0014-3820.2005.tb01814.x>

Henderson MJ, Huff DD, Yoklavich MM (2020) Deep-sea coral and sponge taxa increase demersal fish diversity and the probability of fish presence. *Front Mar Sci* 7:1–19. <https://doi.org/10.3389/fmars.2020.593844>

Holland LP, Jenkins TL, Stevens JR (2017) Contrasting patterns of population structure and gene flow facilitate exploration of connectivity in two widely distributed temperate octocorals. *Heredity* (Edinb) 119:35–48. <https://doi.org/10.1038/hdy.2017.14>

Iannucci A, Cannicci S, Caliani I, Baratti M, Pretti C, Fratini S (2020) Investigation of mechanisms underlying chaotic genetic patchiness in the intertidal marbled crab *Pachygrapsus marmoratus* (Brachyura: Grapsidae) across the Ligurian Sea. *BMC Evol Biol* 20:1–13

Johnson MS, Black R (1982) Chaotic genetic patchiness in an intertidal limpet, *Siphonaria* sp. *Mar Biol* 70:157–164. <https://doi.org/10.1007/BF00397680>

Jombart T (2008) adegenet: an R package for the multivariate analysis of genetic markers. *Bioinformatics* 24:1403–1405. <https://doi.org/10.1093/bioinformatics/btn129>

Jombart T, Devillard S, Balloux F (2010) Discriminant analysis of principal components: a new method for the analysis of genetically structured populations. *BMC Genet*. <https://doi.org/10.1186/1471-2156-11-94>

Kamvar ZN, Tabima JF, Grunwald NJ (2014) Poppr: an R package for genetic analysis of populations with clonal, partially clonal, and/or sexual reproduction. *PeerJ* 2:e281. <https://doi.org/10.7717/peerj.281>

Kennedy BRC, Cantwell K, Malik M, Kelley C, Potter J, Elliott K, Lobecker E, Gray LM, Sowers D, France S (2019) The unknown and the unexplored: insights into the Pacific deep-sea following NOAA CAPSTONE expeditions. *Front Mar Sci* 6:480. <https://doi.org/10.3389/fmars.2019.00480>

Klekowski EJ, Godfrey PJ (1989) Ageing and mutation in plants. *Nature* 340:389–391. <https://doi.org/10.1038/340389a0>

Konopiński MK (2020) Shannon diversity index: a call to replace the original Shannon's formula with unbiased estimator in the population genetics studies. *PeerJ*. <https://doi.org/10.7717/peerj.9391>

Ledoux JB, Mokhtar-Jamaï K, Roby C, Féral JP, Garrabou J, Aurelle D (2010) Genetic survey of shallow populations of the Mediterranean red coral [*Corallium rubrum* (Linnaeus, 1758)]: New insights into evolutionary processes shaping nuclear diversity and implications for conservation. *Mol Ecol* 19:675–690. <https://doi.org/10.1111/j.1365-294X.2009.04516.x>

Levin LA, Le BN (2015) The deep ocean under climate change. *Science* 350:766–768. <https://doi.org/10.1126/science.aad0126>

Lippe C, Dumont P, Bernatchez L (2006) High genetic diversity and no inbreeding in the endangered copper redhorse, *Moxostoma hubbsi* (Catostomidae, Pisces): the positive sides of a long generation time. *Mol Ecol* 15:1769–1780

Long DJ, Baco AR (2014) Rapid change with depth in megabenthic structure-forming communities of the Makapu'u deep-sea coral bed. *Deep Sea Res Part II* 99:158–168. <https://doi.org/10.1016/j.dsr2.2013.05.032>

Luikart G, Ryman N, Tallmon DA, Schwartz MK, Allendorf FW (2010) Estimation of census and effective population sizes: The increasing usefulness of DNA-based approaches. *Conserv Genet* 11:355–373. <https://doi.org/10.1007/s10592-010-0050-7>

Lundsten L, Barry JP, Cailliet GM, Clague DA, DeVogelaere AP, Gel ler JB (2009) Benthic invertebrate communities on three seamounts off southern and central California, USA. *Mar Ecol Prog Ser* 374:23–32. <https://doi.org/10.3354/meps07745>

McClain CR, Lundsten L (2015) Assemblage structure is related to slope and depth on a deep offshore Pacific seamount chain. *Mar Ecol* 36:210–220. <https://doi.org/10.1111/maec.12136>

McClain CR, Lundsten L, Barry J, DeVogelaere A (2010) Assemblage structure, but not diversity or density, change with depth on a northeast Pacific seamount. *Mar Ecol* 31:14–25. <https://doi.org/10.1111/j.1439-0485.2010.00367.x>

Mejía-Mercado BE, Mundy B, Baco AR (2019) Variation in the structure of the deep-sea fish assemblages on Necker Island, Northwestern Hawaiian Islands. *Deep Sea Res Part I: Oceanograph Res Papers* 152:103086. <https://doi.org/10.1016/j.dsr.2019.103086>

Miller KJ, Gunasekera RM (2017) A comparison of genetic connectivity in two deep sea corals to examine whether seamounts are isolated islands or stepping stones for dispersal. *Sci Rep* 7:1–14. <https://doi.org/10.1038/srep46103>

Miller KJ, Rowden AA, Williams A, Häussermann V (2011) Out of their depth? isolated deep populations of the cosmopolitan coral *desmophyllum dianthus* may be highly vulnerable to environmental change. *PLoS One*. <https://doi.org/10.1371/journal.pone.0019004>

Mokhtar-Jamaï K, Pascual M, Ledoux JB, Coma R, Féral JP, Garrabou J, Aurelle D (2011) From global to local genetic structuring in the red gorgonian *Paramuricea clavata*: The interplay between oceanographic conditions and limited larval dispersal. *Mol Ecol* 20:3291–3305. <https://doi.org/10.1111/j.1365-294X.2011.05176.x>

Morato T, González-Irusta JM, Dominguez-Carrió C, Wei CL, Davies A, Sweetman AK, Taranto GH, Beazley L, García-Alegre A, Grehan A, Laffargue P, Murillo FJ, Sacau M, Vaz S, Kenchington E, Arnaud-Haond S, Callery O, Chimienti G, Cordes E, Egildsdottir H, Freiwald A, Gasbarro R, Gutiérrez-Zárate C, Gianni M, Gilkinson K, Wareham Hayes VE, Hebbeln D, Hedges K, Henry LA, Johnson D, Koen-Alonso M, Lirette C, Mastrototaro F, Menot L, Molodtsova T, Durán Muñoz P, Orejas C, Pennino MG, Puerta P, Ragnarsson S, Ramiro-Sánchez B, Rice J, Rivera J, Roberts JM, Ross SW, Rueda JL, Sampaio Í, Snelgrove P, Stirling D, Treble MA, Urrea J, Vad J, van Oevelen D, Watling L, Walkusz W, Wienberg C, Woillez M, Levin LA, Carreiro-Silva M (2020) Climate-induced changes in the suitable habitat of cold-water corals and commercially important deep-sea fishes in the North Atlantic. *Glob Chang Biol* 26:2181–2202. <https://doi.org/10.1111/gcb.14996>

Morgan NB, Cairns S, Reiswig H, Baco AR (2015) Benthic megafaunal community structure of cobalt-rich manganese crusts on Necker Ridge. *Deep Sea Res 1 Oceanogr Res Pap*. <https://doi.org/10.1016/j.dsr.2015.07.003>

Morgan NB, Goode S, Roark EB, Baco AR (2019) Fine scale assemblage structure of benthic invertebrate megafauna on the North Pacific Seamount Mokumanamana. *Front Mar Sci*. <https://doi.org/10.3389/fmars.2019.00715>

Morse JW, Andersson AJ, Mackenzie FT (2006) Initial responses of carbonate-rich shelf sediments to rising atmospheric pCO<sub>2</sub> and "ocean acidification": Role of high Mg-calcites. *Geochim Cosmochim Acta* 70:5814–5830

Mortensen PB, Buhl-Mortensen L (2004) Distribution of deep-water gorgonian corals in relation to benthic habitat features in the Northeast Channel (Atlantic Canada). *Mar Biol* 144:1223–1238. <https://doi.org/10.1007/s00227-003-1280-8>

OBIS (2021) Ocean Biodiversity Information System. In: Intergovernmental Oceanographic Commission of UNESCO

Paradis E (2010) pegas: an R package for population genetics with an integrated–modular approach. *Bioinformatics* 26:419–420. <https://doi.org/10.1093/bioinformatics/btp696>

Parrish FA (2007) Density and habitat of three deep-sea corals in the lower Hawaiian chain. *Bull Mar Sci* 81:185–194

Parrish FA, Baco AR (2007) State of deep coral ecosystems in the US Pacific Islands region: Hawaii and the US Pacific Territories. In: Lumsden SE, Hourigan TF, Bruckner AW, Dorr G (Eds). National Oceanic and Atmospheric Administration, pp 115–194

Parrish FA, Oliver TA (2020) Comparative observations of current flow, tidal spectra, and scattering strength in and around Hawaiian deep-sea coral patches. *Front Mar Sci* 7:1–16. <https://doi.org/10.3389/fmars.2020.00310>

Parrish FA, Grigg RW, DeMello JK, Montgomery AD (2009) The Status of *Corallium* spp. in Hawaii and the US Pacific: Population Status, Trends and Threats, Fisheries, Trade, Management, enforcement and conservation. In: Bruckner AW, Roberts GG (Eds). Citeseer, Silver Springs, MD, pp 87–98

Parrish FA, Baco AR, Kelley C, Reiswig H (2015) State of Deep-Sea Coral and Sponge Ecosystems of the U.S. Pacific Islands Region (Chapter 7). In: Hourigan TF, Etnoyer PJ, Cairns SD (Eds). NOAA Technical Report, pp 1–38

Pérez-Portela R, Cerro-Gálvez E, Taboada S, Tidu C, Campillo-Campbell C, Mora J, Riesgo A (2016) Lonely populations in the deep: genetic structure of red gorgonians at the heads of submarine canyons in the north-western Mediterranean Sea. *Coral Reefs* 35:1013–1026. <https://doi.org/10.1007/s00338-016-1431-2>

Pham CK, Vandeperre F, Menezes G, Porteiro F, Isidro E, Morato T (2015) The importance of deep-sea vulnerable marine ecosystems for demersal fish in the Azores. *Deep Sea Res 1 Oceanogr Res Pap* 96:80–88. <https://doi.org/10.1016/j.dsr.2014.11.004>

Podani J, Miklós I (2002) Resemblance coefficients and the horseshoe effect in principal coordinates analysis. *Ecology* 83:3331–3343. [https://doi.org/10.1890/0012-9658\(2002\)083\[3331:RCATHE\]2.0.CO;2](https://doi.org/10.1890/0012-9658(2002)083[3331:RCATHE]2.0.CO;2)

Qiu B, Koh DA, Lumpkin C, Flament P (1997) Existence and formation mechanism of the North Hawaiian Ridge current. *J Phys Oceanogr* 27:431–444. [https://doi.org/10.1175/1520-0485\(1997\)027%3c431:EAFMOT%3e2.0.CO;2](https://doi.org/10.1175/1520-0485(1997)027%3c431:EAFMOT%3e2.0.CO;2)

Quattrini AM, Baums IB, Shank TM, Morrison CL, Cordes EE (2015) Testing the depth-differentiation hypothesis in a deepwater octocoral. *Proceed Biol Sci Royal Soc* 282:20150008. <https://doi.org/10.1098/rspb.2015.0008>

R Core Team (2018) R: A language and environment for statistical computing. R Foundation for Statistical Computing, Vienna, Austria 3:5

Raymond M, Rousset F (1995) GENEPOP (Version-1.2) - Population-genetics software for exact tests and ecumenicism. *J Hered* 86:248–249

Rivera MAJ, Andrews KR, Kobayashi DR, Wren JLK, Kelley C, Roderrick GK, Toonen RJ (2011) Genetic analyses and simulations of larval dispersal reveal distinct populations and directional connectivity across the range of the Hawaiian Grouper (*Epinephelus quernus*). *J Mar Biol* 2011:1–11. <https://doi.org/10.1155/2011/765353>

Roark EB, Guilderson TP, Flood-Page S, Dunbar RB, Ingram BL, Fallon SJ, McCulloch M (2005) Radiocarbon-based ages and growth rates of bamboo corals from the Gulf of Alaska. *Geophys Res Lett* 32:L04606. <https://doi.org/10.1029/2004GL021919>

Roark EB, Guilderson TP, Dunbar RB, Ingram BL (2006) Radiocarbon-based ages and growth rates of Hawaiian deep-sea corals. *Marine Ecol Prog Series* 327:1–37. <https://doi.org/10.3354/meps327001>

Roark EB, Guilderson TP, Dunbar RB, Fallon SJ, Mucciarone DA (2009) Extreme longevity in proteinaceous deep-sea corals. *Proc Natl Acad Sci USA* 106:5204–5208. <https://doi.org/10.1073/pnas.0810875106>

Rogers AD, Baco A, Griffiths H, Hart T, Hall-Spencer JM (2007) Corals on seamounts. In: Pitcher TJ, Morato T, Hart PJB, Clark MR, Haggan N, Santos RS (Eds). Blackwell Publishing, Oxford, UK, pp 141–169

Rousset F (2008) Genepop'007: a complete re-implementation of the genepop software for Windows and Linux. *Mol Ecol Resour* 8:103–106. <https://doi.org/10.1111/j.1471-8286.2007.01931.x>

Ryman N, Palm S (2006) POWSIM: A computer program for assessing statistical power when testing for genetic differentiation. *Mol Ecol Notes* 6:600–602. <https://doi.org/10.1111/j.1471-8286.2006.01378.x>

Santangelo G, Carletti E, Maggi E, Bramanti L (2003) Reproduction and population sexual structure of the overexploited Mediterranean red coral *Corallium rubrum*. *Mar Ecol Prog Ser* 248:99–108

Sautya S, Ingole B, Ray D, Stöhr S, Samudrala K, Raju KAK, Mudholkar A (2011) Megafaunal community structure of Andaman seamounts including the Back-arc Basin—a quantitative exploration from the Indian Ocean. *PLoS One* 6:e16162. <https://doi.org/10.1371/journal.pone.0016162>

Schlacher TA, Baco AR, Rowden AA, O’Hara TD, Clark MR, Kelley C, Dower JF (2014) Seamount benthos in a cobalt-rich crust region of the central Pacific: conservation challenges for future seabed mining. *Divers Distrib* 20:491–502. <https://doi.org/10.1111/ddi.12142>

Selkoe KA, Henzler CM, Gaines SD (2008) Seascape genetics and the spatial ecology of marine populations. *Fish Fish* 9:363–377

Selkoe KA, Gaggiotti OE, Bowen BW, Toonen RJ (2014) Emergent patterns of population genetic structure for a coral reef community. *Mol Ecol* 23:3064–3079. <https://doi.org/10.1111/mec.12804>

Skillings DJ, Bird CE, Toonen RJ (2011) Gateways to Hawai’i: genetic population structure of the tropical sea cucumber *Holothuria atra*. *J Mar Biol* 2011:1–16. <https://doi.org/10.1155/2011/783030>

Stocks K (2004) Seamount invertebrates: Composition and vulnerability to fishing. In: Pauly D (ed) Morato T. Fisheries Centre, University of British Columbia, pp 17–24

Stocks KI, Hart PJB (2007) Biogeography and biodiversity of seamounts. In: Pitcher T, Morato T, Hart PJB, Clark MR, Haggan N, Santos RS (Eds). Wiley, Blackwell, Hoboken, N.J., pp 255–281

Sweetman AK, Thurber AR, Smith CR, Levin LA, Mora C, Wei C-L, Gooday AJ, Jones DOB, Rex M, Yasuhara M (2017) Major impacts of climate change on deep-sea benthic ecosystems. *Elementa: Sci Anthropolocene* 5:Art. No. 4. <https://doi.org/10.1525/elementa.203>

Takata K, Iwase F, Iguchi A, Yuasa H, Taninaka H, Iwasaki N, Uda K, Suzuki T, Nonaka M, Kikuchi T, Yasuda N (2021) Genome-wide SNP data revealed notable spatial genetic structure in the deep-sea precious coral *Corallium japonicum*. *Front Mar Sci*. <https://doi.org/10.3389/fmars.2021.667481>

Thompson A, Sanders J, Tandstad M, Carocci F, Fuller J (2016) Vulnerable marine ecosystems: Processes and practices in the high seas. FAO Fisheries and Aquaculture Technical Paper 200

Thresher R, Althaus F, Adkins J, Gowlett-Holmes K, Alderslade P, Dowdney J, Cho W, Gagnon A, Staples D, McEnnulty F, Williams A (2014) Strong Depth-Related Zonation of Megabenthos on a Rocky Continental Margin (~700–4000 m) off Southern Tasmania, Australia. *PLoS One* 9:e85872. <https://doi.org/10.1371/journal.pone.0085872>

Toonen RJ, Andrews KR, Baums IB, Bird CE, Concepcion GT, Daly-Engel T, Eble JA, Faucci A, Gaither MR, Iacchei M (2011) Defining boundaries for ecosystem-based management: a multispecies case study of marine connectivity across the Hawaiian Archipelago. *J Mar Biol* 2011:1–13. <https://doi.org/10.1155/2011/460173>

Torrents O, Garrabou J, Marschal C, Harmelin JG (2005) Age and size at first reproduction in the commercially exploited red coral *Corallium rubrum*(L.) in the Marseilles area (France, NW Mediterranean). *Biol Conserv* 121:391–397

Tremel EA, Halpin PN, Urban DL, Pratson LF (2008) Modeling population connectivity by ocean currents, a graph-theoretic approach for marine conservation. *Landsc Ecol* 23:19–36. <https://doi.org/10.1007/s10980-007-9138-y>

Tsounis G, Rossi S, Aranguren M, Gili J-M, Arntz W (2006) Effects of spatial variability and colony size on the reproductive output and gonadal development cycle of the Mediterranean red coral (*Corallium rubrum* L.). *Mar Biol* 148:513–527

Tu T-H, Dai C-F, Jeng M-S (2016) Taxonomic revision of Coralliidae with descriptions of new species from New Caledonia and the Hawaiian Archipelago. *Mar Biol Res* 12:1003–1038. <https://doi.org/10.1080/17451000.2016.1241411>

UN General Assembly (2005) Resolution 59/25: sustainable fisheries, including through the 1995 agreement for the implementation of the provisions of the United Nations Convention on the Law of the Sea of 10 December 1982 Relating to the Conservation and Management of Straddling F

UN General Assembly (2007) Resolution 61/105 Sustainable fisheries, including through the 1995 Agreement for the Implementation of the Provisions of the United Nations Convention on the Law of the Sea of 10 December 1982 relating to the Conservation and Management of Straddling Fis. UNGA A/RES/61/105 paragraph 83(c)

UN General Assembly (2010) Resolution 64/72: Sustainable Fisheries, Including Through the 1995 Agreement for the Implementation of the Provisions of the United Nations Convention on the Law of the Sea of 10 December 1982 relating to the Conservation and Management of Straddling F.

Vaquer-Sunyer R, Duarte CM (2008) Thresholds of hypoxia for marine biodiversity. *Proc Natl Acad Sci USA* 105:15452–15457. <https://doi.org/10.1073/pnas.0803833105>

Wahlund S (1928) The combination of populations and the appearance of correlation examined from the standpoint of the study of heredity. *Hereditas* 11:65–106

Waller RG, Baco AR (2007) Reproductive morphology of three species of deep-water precious corals from the Hawaiian Archipelago: *Gerardia* sp., *Corallium secundum*, and *Corallium lauense*. *Bull Mar Sci* 81:533–542

Weinbauer MG, Brandstätter F, Velimirov B (2000) On the potential use of magnesium and strontium concentrations as ecological

indicators in the calcite skeleton of the red coral (*Corallium rubrum*). *Mar Biol* 137:801–809

Williams A, Schlacher TA, Rowden AA, Althaus F, Clark MR, Bowden DA, Stewart R, Bax NJ, Consalvey M, Kloser RJ (2010) Seamount megabenthic assemblages fail to recover from trawling impacts. *Mar Ecol* 31:183–199. <https://doi.org/10.1111/j.1439-0485.2010.00385.x>

Willis SC, Hollenbeck CM, Puritz JB, Gold JR, Portnoy DS (2017) Haplotyping RAD loci: an efficient method to filter paralogs and account for physical linkage. *Mol Ecol Resour* 17:955–965

Winter DJ (2012) MMOD: an R library for the calculation of population differentiation statistics. *Mol Ecol Resour* 12:1158–1160. <https://doi.org/10.1111/j.1755-0998.2012.03174.x>

Wren JK, Kobayashi DR, Jia Y, Toonen RJ (2016) Modeled population connectivity across the Hawaiian Archipelago. *PLoS ONE* 11:1–25. <https://doi.org/10.1371/journal.pone.0167626>

Wright EP, Kemp K, Rogers AD, Yesson C (2015) Genetic structure of the tall sea pen *Funiculina quadrangularis* in NW Scottish sea lochs. *Mar Ecol* 36:659–667. <https://doi.org/10.1111/maec.12174>

Yesson C, Wright E, Braga-Henriques A (2018) Population genetics of *Narella versluysi* (Octocorallia: Alcyonacea, Primnoidae) in the Bay of Biscay (NE Atlantic). *Mar Biol* 165:1–12. <https://doi.org/10.1007/s00227-018-3394-z>

Zahl S (1977) Jackknifing an index of diversity. *Ecology* 58:907–913

**Publisher's Note** Springer Nature remains neutral with regard to jurisdictional claims in published maps and institutional affiliations.

Springer Nature or its licensor (e.g. a society or other partner) holds exclusive rights to this article under a publishing agreement with the author(s) or other rightsholder(s); author self-archiving of the accepted manuscript version of this article is solely governed by the terms of such publishing agreement and applicable law.